

AD-A271 819



RT DOCUMENTATION PAGE

1a. SECURITY CLASSIFICATION Unclassified		1b. RESTRICTIVE MARKINGS	
2a. DECLASSIFICATION/DOWNGRADING SCHEDULE		3. DISTRIBUTION/AVAILABILITY OF REPORT APPROVED FOR PUBLIC RELEASE: DISTRIBUTION UNLIMITED	
4. PERFORMING ORGANIZATION REPORT NUMBER(S)		5. MONITORING ORGANIZATION REPORT NUMBER(S)	
6a. NAME OF PERFORMING ORGANIZATION Department of Chemistry University of Denver	6b. OFFICE SYMBOL (If applicable)	7a. NAME OF MONITORING ORGANIZATION AFOSR	
6c. ADDRESS (City, State and ZIP Code) Denver, Colorado 80203		7b. ADDRESS (City, State and ZIP Code) 110 DUNCAN AVENUE SUITE B115 BOLLING AFB DC 20332-0001	
8a. NAME OF FUNDING/SPONSORING ORGANIZATION AFOSR/NC	8b. OFFICE SYMBOL (If applicable)	9. PROCUREMENT INSTRUMENT IDENTIFICATION NUMBER AFOSR-90-0259	
8c. ADDRESS (City, State and ZIP Code) 110 Duncan Avenue, Suite B115 Bolling AFB, DC 20332-0001		10. SOURCE OF FUNDING NOS.	
		PROGRAM ELEMENT NO. 61102F	PROJECT NO. 2303
		TASK NO. ES	WORK UNIT NO.
11. TITLE (Include Security Classification) Physical Chemistry of Energetic Nitrogen Compounds			
12. PERSONAL AUTHOR(S) Robert D. Coombe			
13a. TYPE OF REPORT Final Report	13b. TIME COVERED FROM 01-5-91 TO 31-7-93	14. DATE OF REPORT (Yr., Mo., Day) 1 October 93	15. PAGE COUNT
16. SUPPLEMENTARY NOTATION			
17. COSATI CODES		18. SUBJECT TERMS (Continue on reverse if necessary and identify by block number)	
FIELD	GROUP	SUB. GR.	
		azides, isocyanates, amines, nitrenes, aminyl radicals, metastables, photodissociation, energy transfer, reactions, excited states, lasers, thin films.	
19. ABSTRACT (Continue on reverse if necessary and identify by block number)			
<p>This research program produced detailed information concerning the reactions of atoms with azide radicals, amines, aminyl radicals, and isocyanates. These processes release substantial amounts of energy and are constrained (by angular momentum conservation) to generate products in specific states. In addition, reactions and energy transfer processes involving excited nitrene radicals were studied and the rates and mechanisms of several such processes were determined. The information generated provides insight into the fundamental behavior of nitrogen-halogen systems, and is relevant to the development of new lasers.</p>			
20. DISTRIBUTION/AVAILABILITY OF ABSTRACT UNCLASSIFIED/UNLIMITED <input checked="" type="checkbox"/> SAME AS RPT. <input type="checkbox"/> DTIC USERS <input type="checkbox"/>		21. ABSTRACT SECURITY CLASSIFICATION Unclassified	
22a. NAME OF RESPONSIBLE INDIVIDUAL Dr Michael R. Berman		22b. TELEPHONE NUMBER (Include Area Code) (202) 767-4963	22c. OFFICE SYMBOL NC

CONTENTS

I.	Introduction	1
II.	Azide Chemistry	2
III.	Reactions and Photochemistry of Isocyanates	9
IV.	The Chemistry of Halogen Amines	14
	1. The Reaction of Hydrogen Atoms with NCl_3	14
	2. Hydrogen and Deuterium Atom Reactions with NFCI_2	15
	3. The Reaction of H Atoms with NF_2Cl	22
V.	Reactions and Energy Transfer Processes of Excited Nitrenes	25
	1. Energy Transfer from $\text{NCl}(a^1\Delta)$ to Iodine Atoms	25
	2. $\text{NCl}(a^1\Delta)$ Quenching by Diatomics	31
	3. Reactions of $\text{NH}(a^1\Delta)$ with Molecular Halogens	38
VI.	Photochemical Deposition of IIB-VI Thin Films	43
VII.	Publications Arising from This Work	47
VIII.	Personnel	48
IX.	References	49

93-26629



055

I. Introduction

This report describes the results of research performed during the period 1 May 1990 through 31 July 1993 under the auspices of AFOSR grant no. AFOSR - 90 - 0259. The program, entitled "Physical Chemistry of Energetic Nitrogen Compounds" has as its global objectives elucidation of the mechanisms of energy storage in highly energetic or metastable molecules, and understanding of the constraints on the energy flow when such species are stimulated by photolysis, reaction, or collisional energy transfer. This program represents the last three and one half year period in a research effort spanning several years. Much of this effort, as originally conceived, has involved studies of small nitrogen bearing molecules such as azides, isocyanates, amines, and related radicals such as nitrenes and aminyls. These species are of interest with respect to U.S. Air Force applications in lasers, high energy density materials, new laser systems, and energetic phenomena in the atmosphere.

The program was divided into four general areas of research, which were reactions of azide systems, photochemistry and reactions of isocyanates, halogen amine systems, and reactions and energy transfer processes involving excited nitrene radicals. The research on azides and isocyanates represents the latter part of a long history of work on these systems in our laboratory, and this portion of the program was minimal. The larger part of the program focussed on halogen amines and excited nitrenes. As was shown by the results of this research, these systems are particularly interesting in that the paths for reaction or energy transfer appear to be strongly constrained. Hence, the chemistry of these systems holds much information regarding the details of energy storage and release in nitrogen/halogen

systems. In addition, a number of important applications (particularly in near IR laser systems) may be realized.

In addition to the primary focus of the program on nitrogen/halogen systems, a small part of the effort was diverted to test a novel idea concerning the use of laser-induced chemistry for the deposition of IIB - VI thin films. These films are of interest with respect to Air Force applications in semiconductor devices and optical coatings.

Within each of the research areas, a number of individual projects were performed. Since the results of these projects have in large measure been described in detail in the open literature (see Section VII below), only a brief summary of each project, along with an assessment of the significance of the results, is presented below.

II. Azide Chemistry

Our work on azides focussed on making accurate measurements of rate constants for atom + N₃ reactions, in particular the F + N₃ reaction. The most commonly used method for generating N₃ in the gas phase is the reaction of F atoms with HN₃, a very rapid ($k = 1.5 \times 10^{-10} \text{ cm}^3 \text{ s}^{-1}$) process which produces N₃ and vibrationally excited HF.^{1,2,3} The subsequent reaction of N₃ with F atoms is of particular interest since it produces electronically excited NF(a¹Δ) with a branching fraction near unity³. Data from the first observation of this reaction by Coombe and Pritt¹ indicated a rate constant on the order of $10^{-12} \text{ cm}^3 \text{ s}^{-1}$, based on the time dependence of the NF(a¹Δ) product. This value was supported by later measurements done by David and Coombe,⁴ who determined a rate constant $k = 2 \times 10^{-12} \text{ cm}^3 \text{ s}^{-1}$ from observation of emission from excited N₂, which was

thought to track the N_3 in the system. In 1987, Setser and coworkers³ made an extensive study of the $F + HN_3$ system which included the vibrational distribution of the HF produced in the first step and the branching fraction to $NF(a^1\Delta)$ in the second step. These authors also reported a rate constant for $F + N_3$ based on the $NF(a^1\Delta)$ rise time in their system. Surprisingly, their data indicated a value $4 \pm 2 \times 10^{-11} \text{ cm}^3 \text{ s}^{-1}$, nearly 20 times larger than the previously reported results.

Our experiments sought to resolve the issue of the $F + N_3$ rate constant, and to determine rate constants for other atom + N_3 reactions by competitive rate experiments. The measurements were made by direct observation of N_3 using LIF on its $X^2\Pi - A^2\Sigma^+$ transition near 270 nm.⁵ In the $F + HN_3$ system, the time dependence of the N_3 density, and hence of the LIF intensity, is given by a sum of rising and falling exponential terms corresponding to the rates of the $F + HN_3$ formation reaction and any N_3 removal processes. The latter are dominated by the $F + N_3$ reaction. There is general agreement on the $F + HN_3$ rate constant ($1.5 \times 10^{-10} \text{ cm}^3 \text{ s}^{-1}$), and on the fact that it is larger than that for $F + N_3$. Hence, the rise of the N_3 signal corresponds to the $F + HN_3$ rate, and its decay to $F + N_3$ and other decay processes. Measurement of the N_3 decay rate as a function of the F atom density should unambiguously yield the $F + N_3$ rate constant.

The reaction was established by adding small flows of HN_3 to a stream of F atoms (produced by microwave discharge of Ar flows containing CF_4 , F_2 , or SF_6) in a standard discharge flow reactor. The LIF probe beam (from a frequency doubled excimer laser pumped dye laser) was passed through the flow at a fixed observation point, and the reaction

time was varied by changing the position of the HN_3 injector with respect to the LIF probe. Figure 1 shows a portion of an excitation spectrum of N_3 produced in our experiments. The LIF emission was monitored with a cooled photomultiplier through a filter centered at 270 nm. The spectrum is in very good agreement with that originally published by Setser and co-workers,⁵ but shows more detailed structure.

The greatest problem in the experiments proved to be accurate measurement of F atom flow rates. Ultimately, this was done by a titration in which the F atom flow was monitored via HF emission produced by the admission of ethane downstream. The PMT monitored emission from the $v=3$ to $v=0$ transition in HF near 874 nm. CF_3I was then added upstream of the observation port to remove the F atoms and hence the HF emission signal. At the point at which the HF emission was quenched, the CF_3I flow was equal to the F atom flow.

Figure 2 shows a plot of the measured N_3 decay rate vs. the F atom density, for CF_4 as a source of F atoms. The slope of the plot indicates a rate constant $k = (5.9 \pm 0.6) \times 10^{-11} \text{ cm}^3 \text{ s}^{-1}$ for the $\text{F} + \text{N}_3$ reaction at 295K, in good agreement with a value previously reported by Setser.³ Since we observed in our experiments that the % dissociation of the CF_4 , like the F atom density, varied with the CF_4 flow rate (such that N_3 removal by F atoms could not be distinguished from removal by CF_2), F_2 and SF_6 were also tested as sources of F atoms. These experiments gave similar results for the rate constant at room temperature.

Competitive rate studies were performed by allowing N_3 to react with a mixture of two different atoms, one of which was F. A double concentric sliding injector was used in the flow reactor, to allow two species to be admitted to the flow at a fixed time from one another but at a variable time from the observation point. F atoms were produced in a microwave

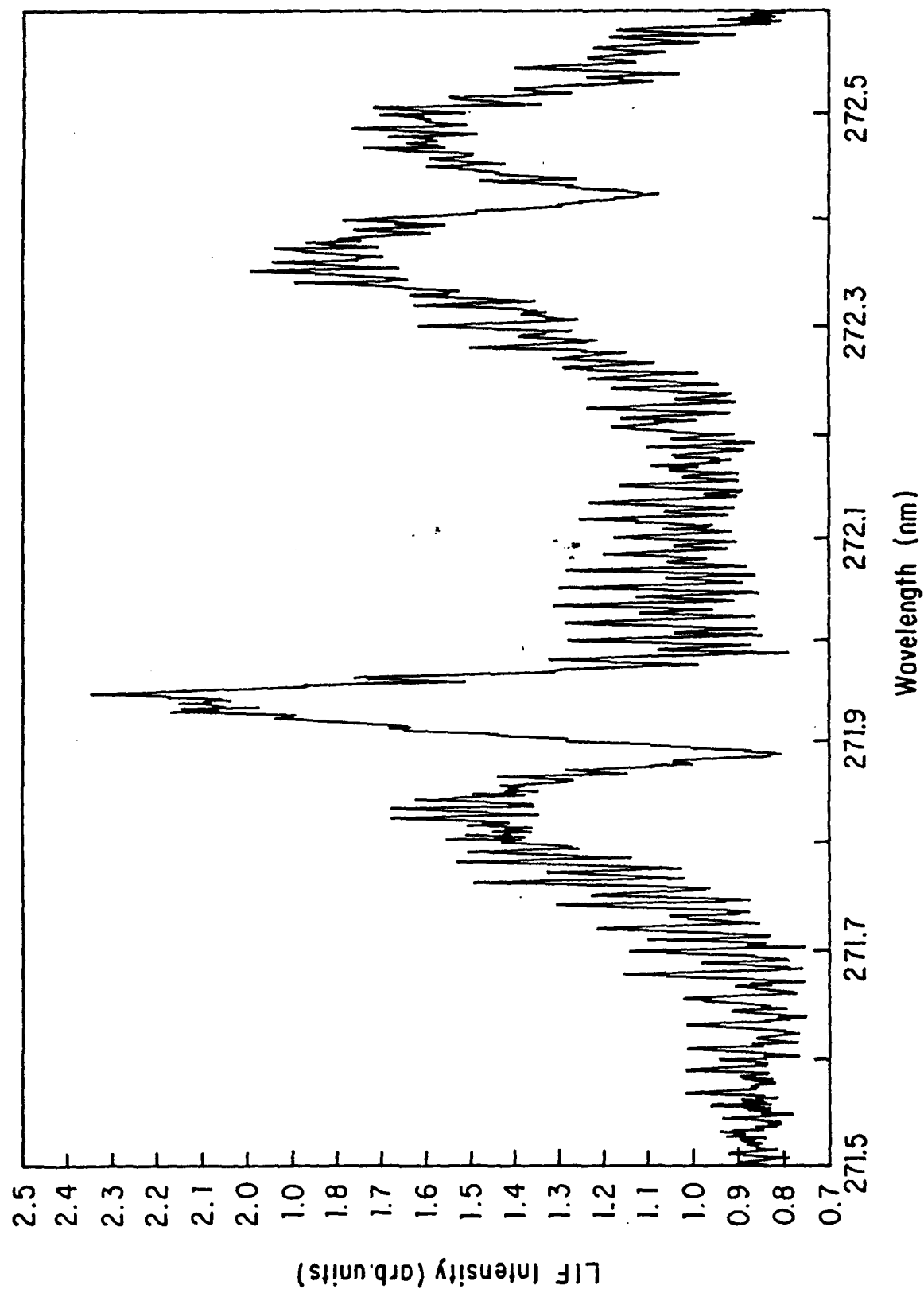


Figure 1. A Portion of the LIF Excitation Spectrum of N_3 Radicals.

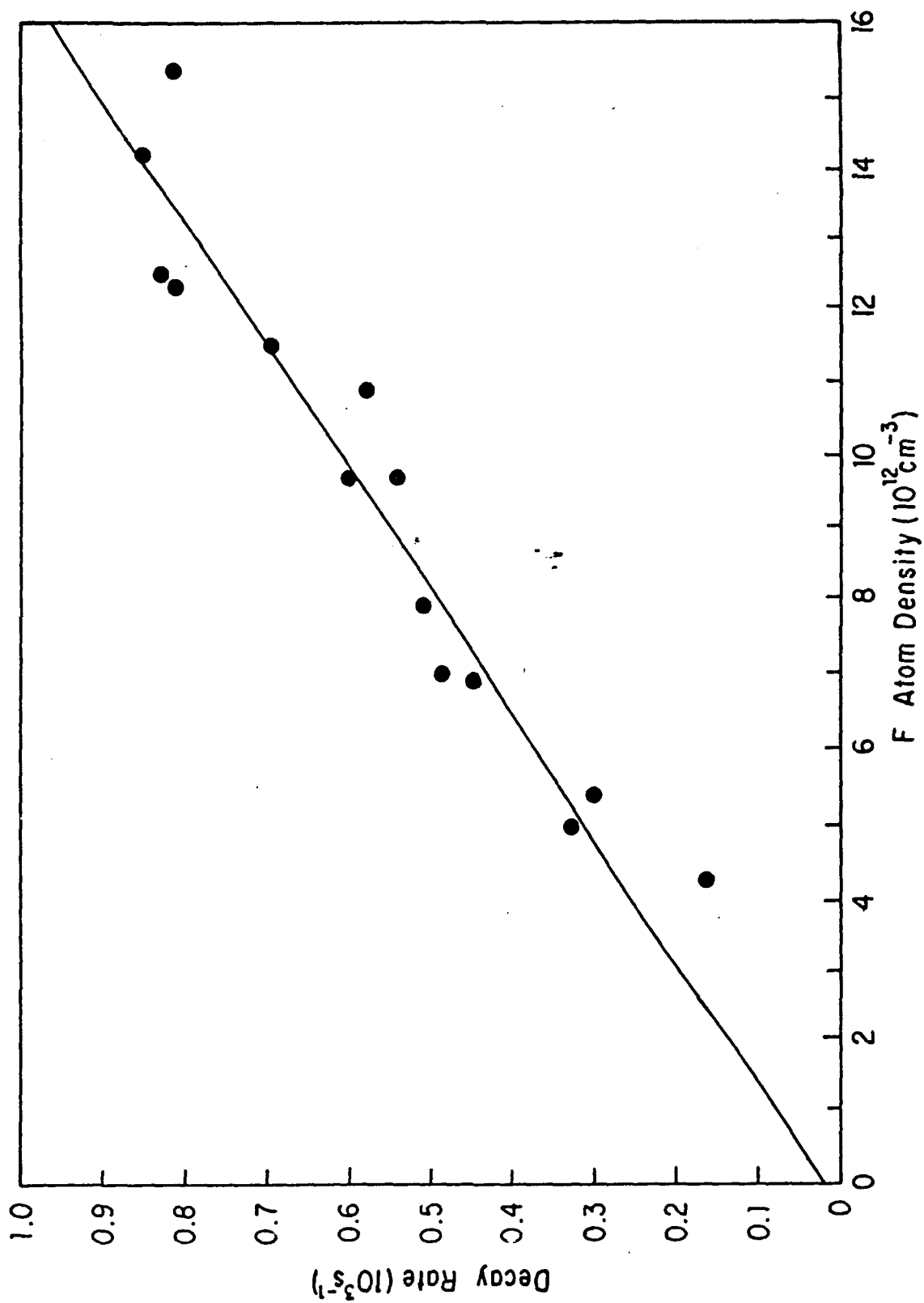


Figure 2. A Plot of the Rate of Decay of N₃ Radicals vs. the density of F Atoms. F Atoms from a Microwave Discharge through CF₄.

discharge as before, and a second atom source (H_2 , Cl_2 , or Br_2) was admitted downstream such that a portion of the F atoms were converted to H, Cl or Br atoms prior to the admission of HN_3 to the flow. When the HN_3 was added, it quickly reacted with the F atoms present to produce N_3 . Subsequently, the mixed atomic species present (F and H, Cl, or Br) compete for reaction with the available N_3 in the stream.

The fraction of the N_3 that reacted with the F atoms was monitored by the intensity of the NF a \rightarrow X emission (874 nm) produced by this reaction. The change in this intensity was then observed upon addition of H_2 , Cl_2 , or Br_2 . The main assumption is that the subsequent decrease in the NF a \rightarrow X intensity is caused by competition between the different atoms for the N_3 . In this case, the intensities can be related to rate constants of the competing reactions by the following expression:

$$\left(\frac{I_0 - I}{I} \right)_{NF} = \frac{k_{Cl}[Cl]}{k_F[F]} \quad (1)$$

where I_0 is the intensity from F atoms alone, I is the intensity from the atom mixture, and k_F and k_{Cl} are rate constants for the $F + N_3$ and $Cl + N_3$ reactions, respectively. Hence, a plot of $(I_0 - I)/I$ vs. $[Cl]/[F]$ should be linear, with a slope given by k_{Cl}/k_F . Figure 3 shows such a plot for the Cl/F competition. The plot is indeed linear and the slope indicates that $k_{Cl}/k_F = 5.6$. From the value for k_{Cl}/k_F is then $2.8 \times 10^{-10} \text{ cm}^3 \text{ s}^{-1}$. Rate constants were similarly determined for the N_3 reactions with H and Br atoms. All of the results are collected in Table I.

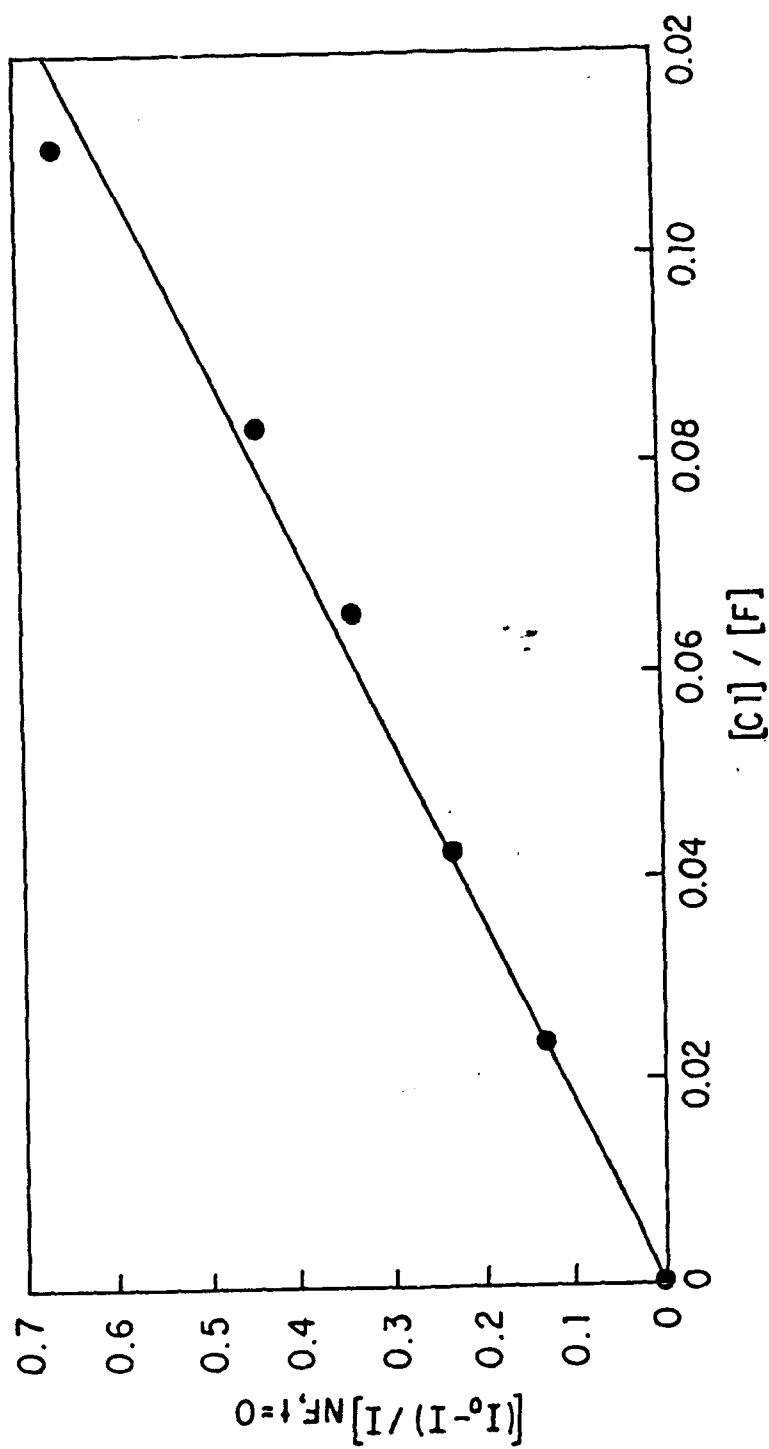


Figure 3. Competitive Rate Plot for the Reaction of N_3 Radicals with F and Cl Atoms.

Table I. Rate Constants for Reactions of N_3 Radicals with Atoms

Reactant Atom	$k(\text{cm}^3\text{s}^{-1})$
F	$5.8 \pm 0.6 \times 10^{-11}$
Cl	$2.8 \pm 0.4 \times 10^{-10}$
H	$1.0 \pm 0.1 \times 10^{-10}$
Br	$3 \pm 2 \times 10^{-10}$

The present data show very clearly that the rate constant for $F + N_3$ is close to the value reported by Habdas and Setser³. They do not support the values from the earlier measurements by Coombe and Pritt,¹ although these authors were correct in their finding that $Cl + N_3$ is about 5 times faster than $F + N_3$. The larger rate constants for H, Cl, and Br atom reactions with N_3 relative to $F + N_3$ must reflect the details of the potential energy surfaces of the intermediate azides HN_3 , ClN_3 , and BrN_3 . Studies of the temperature dependence of these rates would provide information which might be correlated to theoretical treatments of these molecules. We hope to pursue such studies in the future.

III. Reactions and Photochemistry of Isocyanates

Previous experiments in our laboratory⁶ have shown that the reaction of HNCO with excited $O(^1D)$ atoms proceeds by electrophilic attack by oxygen on the -NCO chain, generating NH and CO_2 as the primary products. Remarkably, this process conserves spin and the product NH is formed almost exclusively in its excited $a^1\Delta$ state. As a part of this program, we performed analogous experiments with the reaction of $O(^1D)$ atoms with CINCO. If the mechanism were the same in this case, this reaction might offer a useful

source of $\text{NCl}(a^1\Delta)$ metastables. On the other hand, if the reaction were truly dominated by electrophilic attack, production of $\text{ClO} + \text{NCO}$ might be a major channel. Our objective was to measure the rate constant for the reaction and to determine which product channels are dominant.

The experiments involved pulsed photolysis of flowing O_3/CINCO mixtures at 249 nm with a KrF laser. Since the reaction produces no short lived chemiluminescent products, the rate of $\text{O}(^1\text{D})$ quenching in this medium was monitored by admission of an excess density of HNCO . The $\text{O}(^1\text{D}) + \text{HNCO}$ reaction generates⁶ a small yield of $\text{NH}(A^3\Pi)$ which is a short lived emitter at 336 nm. In this case, the $\text{NH } A \rightarrow X$ emission time profile tracks the decay of $\text{O}(^1\text{D})$ in the system. The decays were found to be exponential with rates which varied inversely with the CINCO density, as shown in Figure 4. From the slope of the plot, the rate constant for $\text{O}(^1\text{D})$ quenching by CINCO is determined to be $1.3 \pm 0.2 \times 10^{-10} \text{ cm}^3 \text{ s}^{-1}$, about one third of that for quenching by HNCO .

Many experiments were performed in a search for the production of NCl by the $\text{O}(^1\text{D}) + \text{CINCO}$ reaction. $\text{NCl}(a^1\Delta)$ and $\text{NCl}(b^1\Sigma^+)$ were sought by their characteristic emissions at 1.08 μm and 665 nm, respectively. No emission was found. The sensitivity of these experiments was calibrated by the photolysis of ClN_3 at 249 nm, a process which produces⁷ both the $a^1\Delta$ and $b^1\Sigma^+$ states of NCl . From the calibration, an upper limit for the branching fraction to excited NCl was set at 0.1%. Ground state NCl was sought by LIF on the $X^3\Sigma \rightarrow b^1\Sigma^+$ transition. Here again, no LIF was found. From a comparison with similar experiments on $\text{NF}(X)$ performed by Koffend and coworkers,⁸ the branching fraction to $\text{NCl}(X)$ was determined to be less than 0.1%.

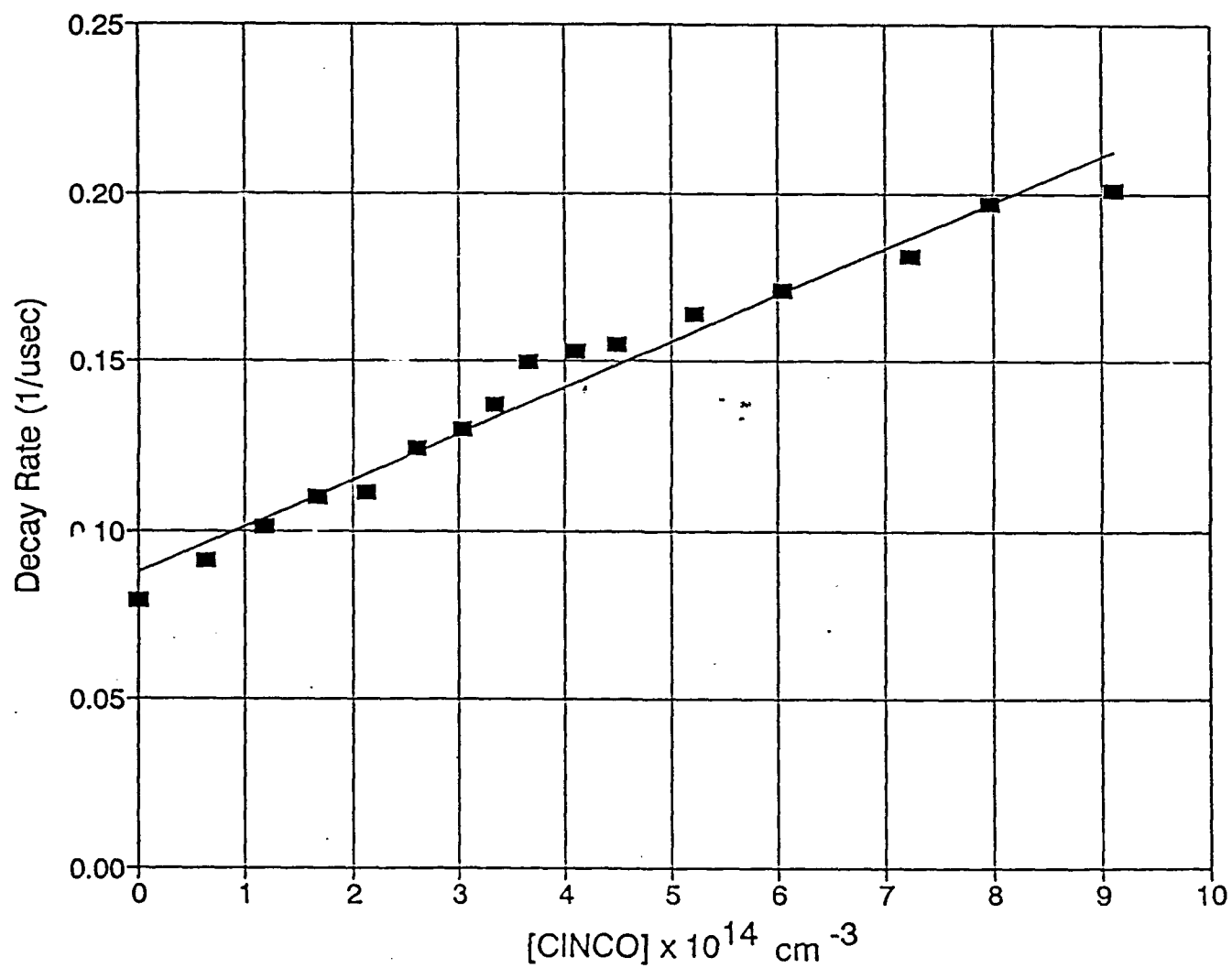


Figure 4. Exponential Decay of the Density of O(¹D) Atoms vs. the Density of CINCO

These results certainly suggest that production of $\text{ClO} + \text{NCO}$ is the dominant channel in the reaction. To probe this possibility, NCO was sought by LIF on its $X^2\Pi \rightarrow A^2\Sigma^+$ transition near 438 nm. Some NCO is produced⁹ by the photolysis of CINCO at 249 nm, and this was readily observed. The time profile of the NCO exhibits a rise and decay corresponding to rotational relaxation in $\text{NCO}(X^2\Pi)$ and overall loss of this radical from the system, respectively. These data are shown in Figure 5. The presence of O_3 results in significant enhancement of the NCO LIF signal, as is shown in the figure. Clearly, NCO is a product of the reaction.

A limit on the branching fraction to NCO was obtained from comparison of the data with a kinetic model for the system. The model included $\text{O}(^1\text{D})$ quenching by various species present as well as rotational relaxation of the NCO product. The absolute density of NCO corresponding to the LIF signals observed was obtained by calibration against the NCO produced by CINCO photodissociation, with the quantum yield set at unity. The modeling results (from numerical integration of the coupled differential rate equations) are shown as solid lines through the data points in Figure 5. Clearly, the agreement is very good. The rise and decay times were a sensitive function of the degree of rotational excitation (65%) and the rate of its relaxation. The absolute intensities were a sensitive function of the branching fraction to $\text{ClO} + \text{NCO}$, found to be 20%. This result represents a lower limit, largely because of the assumption of unity branching fraction to NCO in the photodissociation of CINCO. Indeed, the branching fraction in the $\text{O}(^1\text{D}) + \text{CINCO}$ reaction is likely to be

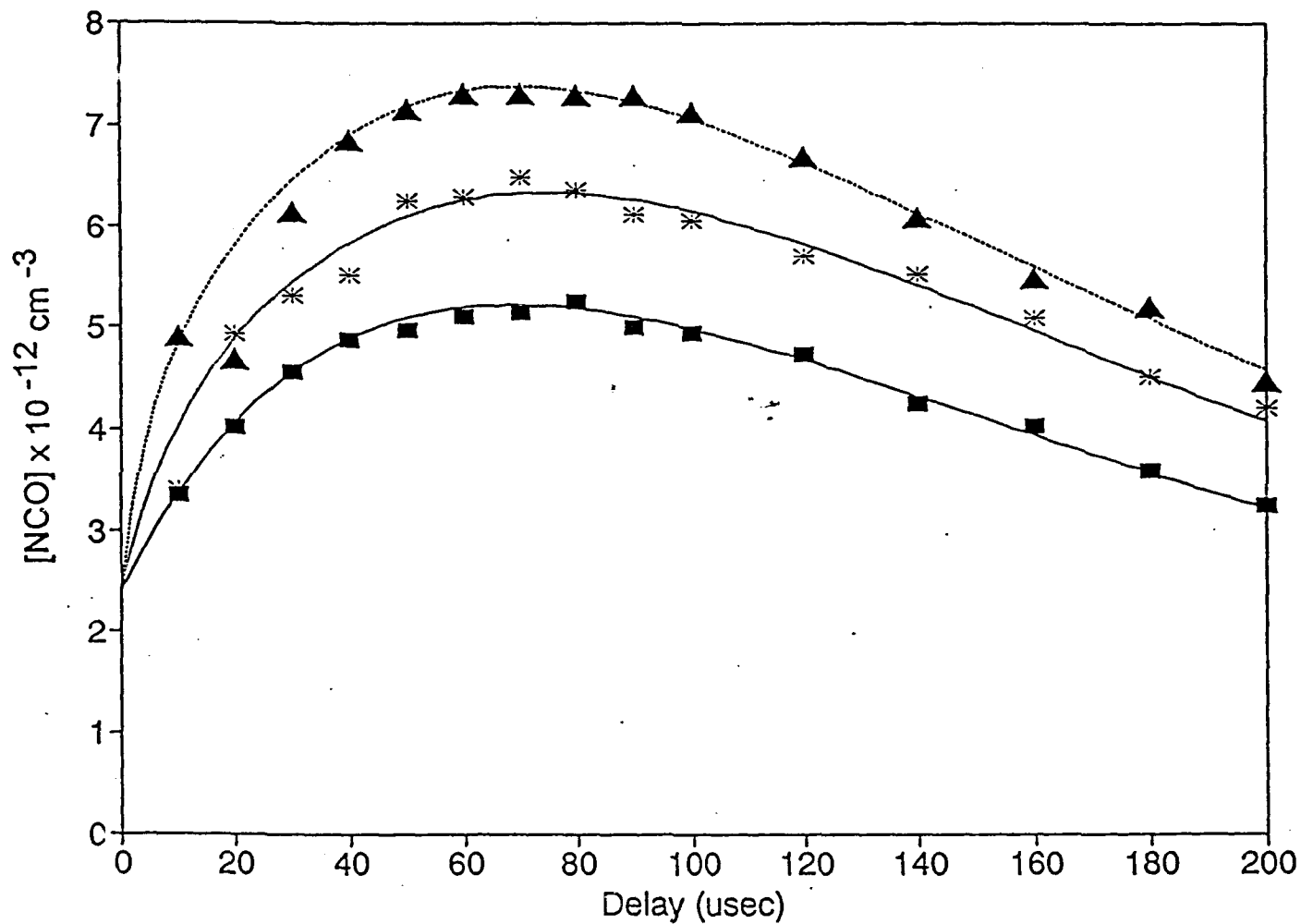


Figure 5. Time Profiles of the Density of NCO Radicals Produced by 248 nm Photolysis of $O_3/ClNCO$ Mixtures. Squares, Photolysis of $ClNCO$ alone. Asterisks and Triangles, photolysis of $ClNCO$ with $[O_3] = 1.7 \times 10^{14} \text{ cm}^{-3}$ and $3.6 \times 10^{14} \text{ cm}^{-3}$. Lines through the Data Are the Results of the Kinetic Model.

much greater than 20%, since the CINCO photolysis is known^{9,10} to produce fragments other than Cl + NCO.

The model indicates that a large fraction of the NCO produced by either CINCO photolysis or the O(¹D) + CINCO reaction is internally excited. Given the time frame of the relaxation of this excitation and the density of the He buffer gas, it seems that the excitation is largely in rotational degrees of freedom. Hence, CINCO photochemistry would appear to offer an excellent opportunity to study the dynamics of rotational relaxation in NCO, an important species in combustion processes.

IV. The Chemistry of Halogen Amines

1. The Reaction of Hydrogen Atoms with NCl₃

Our work on NCl₃ and its reaction with hydrogen atoms represents the conclusion of research begun under the auspices of a previous AFOSR grant (AFOSR - 87 - 0110) and finished during the beginning of the present program. Our interest in halogen amines is based principally on their utility for the generation of excited singlet halogen nitrenes (e.g., a¹Δ and b¹Σ⁺ states of NF or NCl), species which are well known as energy storage agents in chemical laser systems.¹¹ The NCl₃ reaction with excess hydrogen atoms is prototypical.

The mechanism includes two steps, as follows:



The second step is analogous to the well studied¹² H + NF₂ reaction, which proceeds on the single ground state potential energy surface of the HNF₂ intermediate. The amine-like

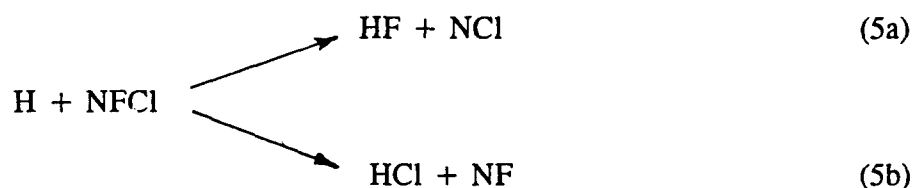
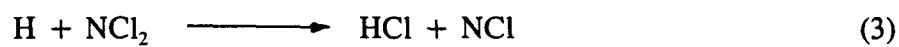
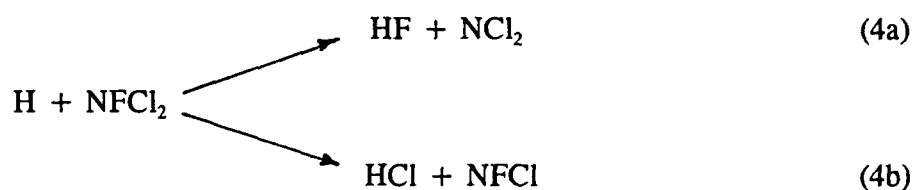
intermediate eliminates the hydrogen halide (a singlet) leaving the nitrene in an excited singlet state. For $H + NF_2$, the yield¹² of $NF(a^1\Delta)$ is 91%. Presumably, reaction (2) above should be similarly constrained, and our experiments have borne this out.

Discharge-flow methods were employed to observe the $H + NCl_3/NCl_2$ reactions and to determine their rate constants. The $a^1\Delta$ and $b^1\Sigma^+$ excited states of NCl were observed by their chemiluminescence at $1.08\ \mu m$ and $565\ nm$, respectively. From the time dependence of this chemiluminescence, the limiting rate constant in the system was determined to be $4.0 \pm 0.4 \times 10^{-12}\ cm^3\ s^{-1}$. Although we originally believed this rate constant to correspond to the first step ($H + NCl_3$), recent data from experiments by Setser and co-workers¹³ have suggested that the second process ($H + NCl_2$) may in fact be slower. The branching fraction to the $a^1\Delta$ state was determined to be $> 15\%$ by calibration of the detection system with the $O + NO$ reaction.¹⁴ This result is a lower limit as it was determined assuming no quenching of the excited NCl and no reaction of NCl_3 or NCl_2 with species other than H atoms. Hence the true branching fraction is likely to be considerably greater than 15% . The branching fraction to the $NCl(b^1\Sigma^+)$ state was found to be very much smaller, 0.015% .

These results indicate that the $H + NCl_3$ system is an interesting and potentially useful source of $NCl(a^1\Delta)$ metastables. Recently, we have shown¹⁵ that this chemical system is very compatible with the generation of excited $I(^2P_{1/2})$ by energy transfer from $NCl(a^1\Delta)$ to iodine atoms, and offers the possibility for an all gas phase iodine laser. The details of this energy transfer process are described in Section V below.

2. Hydrogen and Deuterium Atom Reactions with $NFCl_2$

Although $\text{H} + \text{NCl}_3$ does indeed make $\text{NCl}(a^1\Delta)$, NCl_3 is itself an unstable compound which can be difficult to handle. Seeking to improve on this situation, we performed an extensive series of experiments with the analogous molecule NFCI_2 . This species is much more stable than NCl_3 , it can be purified safely by fractional condensation, and it is storable indefinitely in condensed form or as a gas. Further, reaction with H atoms offers a number of interesting possibilities for branching, as follows:



Hence, this system might well produce excited singlets of both NF and NCl. This is a most interesting possibility, as Benard¹¹ has shown that energy pooling among $\text{NF}(a^1\Delta)$ and $\text{NCl}(a^1\Delta)$ can lead to production of $\text{NF}(b^1\Sigma^+)$, a mechanism which is enhanced by the presence of iodine atoms (which are pumped by $\text{NCl}(a)$ as noted above).

The experiments with NFCl_2 were performed in a manner similar to those with NCl_3 , using a discharge-flow apparatus with detection of visible and near-IR chemiluminescence. Figure 6 shows a typical spectrum obtained in the visible region. Clearly, the system does indeed produce both excited NF and NCl. Chemiluminescence from the $b^1\Sigma^+$ states of NF and NCl is evident in the spectrum, as is the $\text{NF}(a^1\Delta)$ state which emits near 874 nm. Chemiluminescence from $\text{NCl}(a^1\Delta)$ was found as well near 1.08 μm . The time profile of the $\text{NCl } b \rightarrow X$ chemiluminescence was used to probe the kinetics of the system, since the time decay of the $\text{NCl}(b^1\Sigma^+)$ should track the overall rate of formation of NCl in the system. The data indicated a limiting rate constant of $2.6 \pm 0.2 \times 10^{-12} \text{ cm}^3 \text{ s}^{-1}$, about half of that found for the analogous NCl_3 system.

A number of experiments were performed in an effort to determine the relative amounts of $\text{NCl}(a)$ and $\text{NF}(a)$ produced by the system. By calibration of the absolute response of the detection system at 874 nm and 1077 nm (the wavelengths of the NF and NCl transitions), it was determined that the production of $\text{NF}(a)$ is greatly favored. The steady state density of $\text{NF}(a)$ was found to be about an order of magnitude greater than that of $\text{NCl}(a)$, indicating that reaction 4b predominates over 4a, and that 5b predominates over 5a. Subsequent experiments (see below) have indicated that reaction 4 proceeds exclusively to $\text{HCl} + \text{NFCl}$, such that this result is indicative of the relative branching in reaction 5.

Experiments were also performed to investigate the occurrence of second order energy pooling processes in the reaction mixture. In this case, D atoms were used in place of H atoms in the reaction mixture, since it is well known¹⁶ that vibrationally excited HF can pump $\text{NF}(a)$ to $\text{NF}(b)$ by a resonant process which does not occur with DF. Figure 7 shows a plot of the

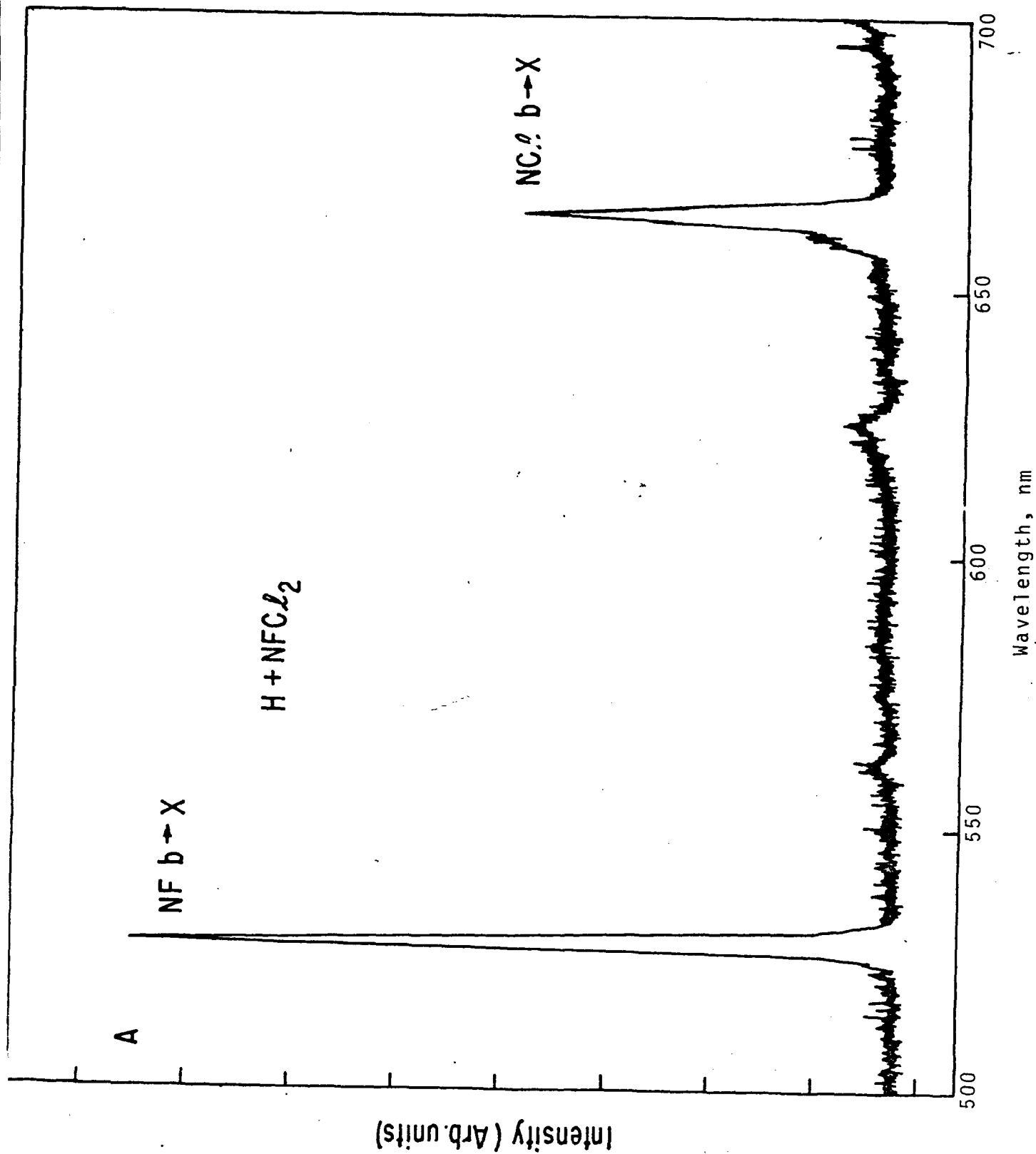


Figure 6. Spectrum of Visible Emission from the Reaction of H Atoms with NFCl_2 .

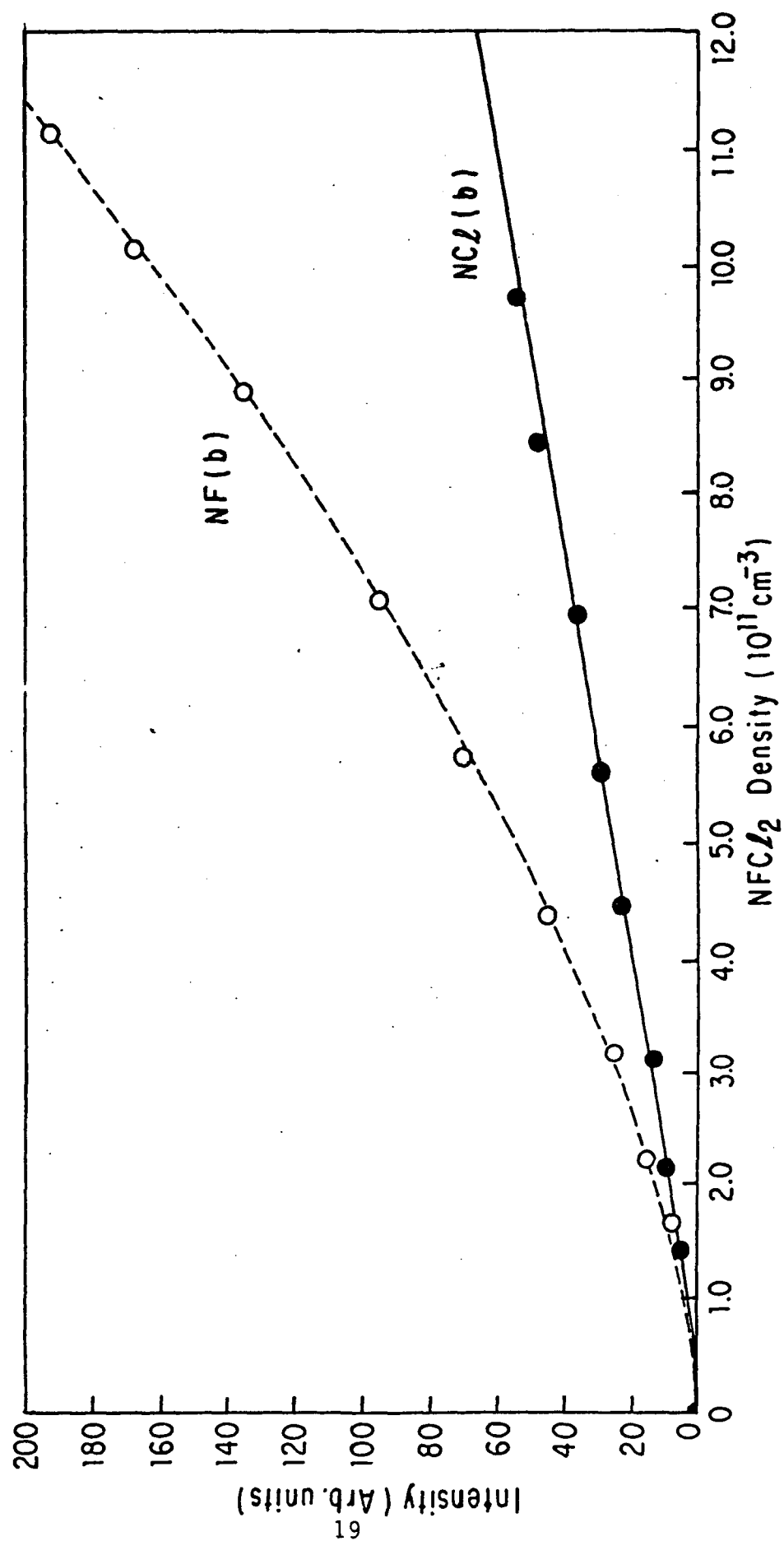


Figure 7. Intensity of Emission from $b^1\Sigma^+$ States of NF and NCl vs. the Initial Density of NFCl_2 .

NF(b) and NCl(b) intensities as a function of the NFCl_2 flow rate. Clearly, NCl(b) increases linearly with the amine flow whereas NF(b) increases in a nonlinear (nearly quadratic) fashion. This result is most suggestive of pumping of NF(b) by an energy pooling process, likely the $\text{NF(a)} + \text{NF(a)}$ mechanism noted above. Very dramatic evidence of this process was obtained when iodine atoms were admitted to the system. This was done by admitting a small flow of HI, such that I atoms were formed by the $\text{F} + \text{HI}$ and $\text{D} + \text{HI}$ reactions. As HI was added, the NF(b) intensity increased by a factor of four, whereas the NF(a) intensity was reduced by 15%, and the NCl(a) intensity was completely quenched. This result (shown in Figure 8) suggests that the NCl(a) density is about 15% of the NF(a) density (in agreement with the data noted above), and that the initial density of NF(b) is about 4% of that of NF(a). The fact that energy pooling processes are observable for the very low reagent densities of our experiments (near 10^{-10} cm^{-3}) testifies to the speed and efficiency of these processes.

More recently, additional data regarding the $\text{H} + \text{NFCl}_2$ system has been obtained in collaboration with Professor D.W. Setser and co-workers at Kansas State University.¹³ These experiments, performed in Dr. Setser's laboratory, focussed on the production of hydrogen halides (HCl and HF) in the system and the vibrational population distributions in these molecules. The experiments were performed with a discharge flow system linked to an FTIR which detected near IR chemiluminescence from vibrationally excited HF and HCl. By varying the flow rates of the H atom and NFCl_2 reagents, the first and second steps in the mechanism could be isolated. These experiments showed that the first step (reaction 4) does proceed exclusively to $\text{HCl(v)} + \text{NFCl}$. Further, it was shown that NF(a) and HCl(v) are indeed the predominant products of the second step, verifying the result noted above. No straightforward

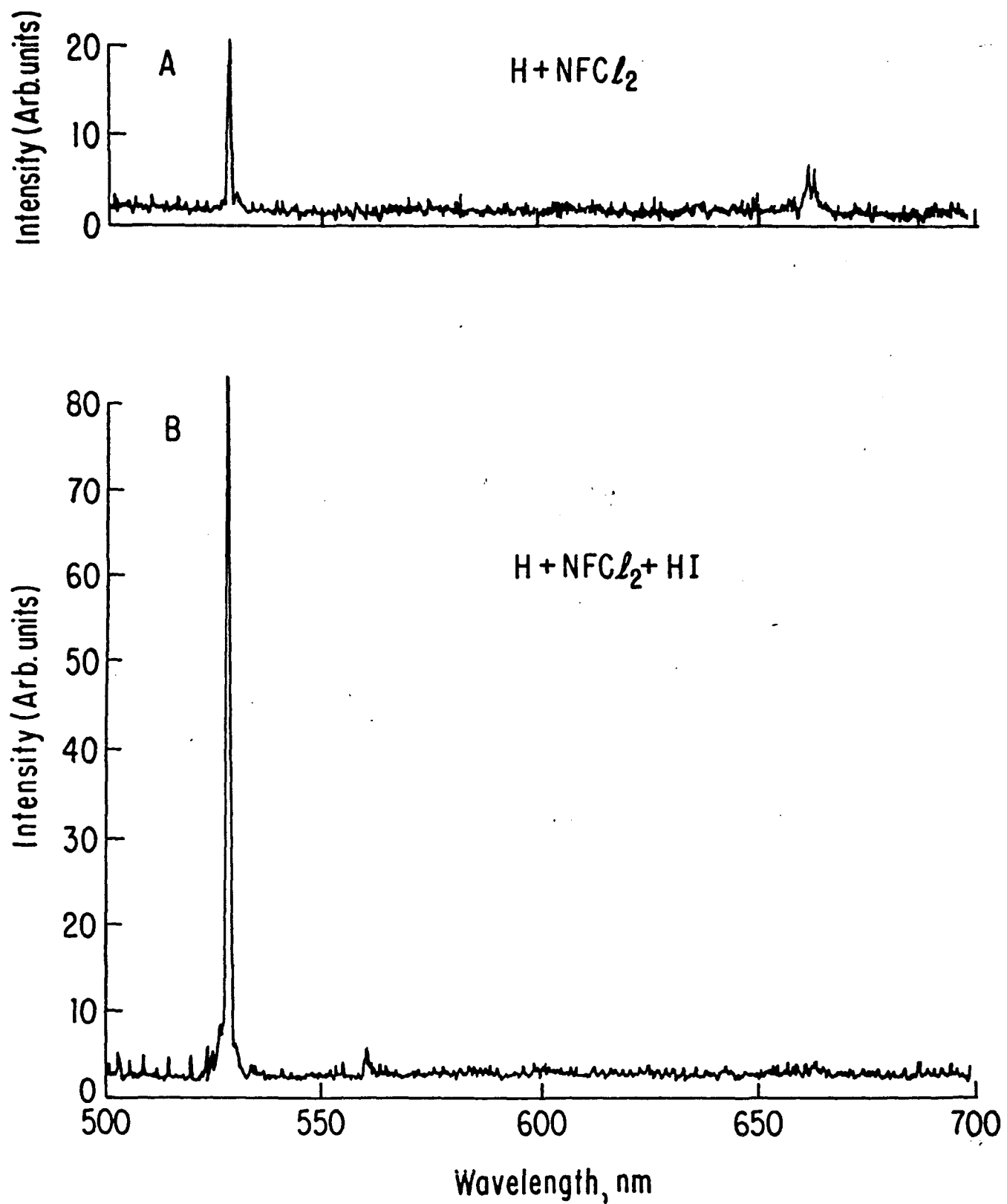


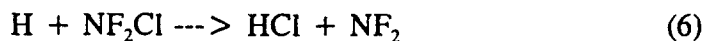
Figure 8. Spectra of Visible Emission from the H + NCF₂ System without Added HI(A) and with Added HI(B).

explanation (beyond speculation) is yet at hand regarding this remarkable selectivity in the system. In both the first and second steps, the paths favored by the reaction are less exothermic than their competitors, and these processes are surely controlled by dynamics. The vibrational distributions in HCl (from the first step) and HF (from the second step) showed that these reactions proceed by abstraction and addition-elimination, respectively.

The experiments at Kansas State also yielded values for the rate constants of the mechanism, which unfortunately do not agree well with the earlier DU results. The IR chemiluminescence data indicated that the rate constant of the first step is near $2 \times 10^{-11} \text{ cm}^3 \text{ s}^{-1}$, and that of the second step is approximately $4 \times 10^{-11} \text{ cm}^3 \text{ s}^{-1}$. At this point, we are not certain where the origin of the disparity lies.

3. The Reaction of H Atoms with NF_2Cl

During the course of the program, we also made a brief investigation of the reaction of H atoms with NF_2Cl . Based on the propensity for H atoms to remove the Cl atoms from NFCl_2 , this reaction is anticipated to be an efficient source of NF_2 radicals, as follows:



Subsequent reaction of the NF_2 radicals with H atoms would generate $\text{NF}(a^1\Delta)$. For this work, samples of NF_2Cl were prepared in the laboratory of Professor J.V. Gilbert (a colleague at DU) and diluted with He to 5% mixtures in 5 liter pyrex bulbs. The reaction of this species with H atoms was studied in a standard discharge-flow reactor. H atoms were generated by reaction of excess H_2 with F atoms from a discharge through CF_4/Ar . Chemiluminescence from the system was monitored with a 0.25 m monochromator and a cooled GaAs PMT. $\text{NF } a \rightarrow X$ and $b \rightarrow X$ emission at 874 and 529 nm, respectively, dominated the spectrum. Weak N_2 first positive

emission was also observed over a wide range in the visible region. Significantly, no emission from NCl (specifically the $b \rightarrow X$ transition near 665 nm) was found, suggesting that reaction 6 does not branch to $\text{HF} + \text{NCl}$, as expected. The N_2 first positive emission is a well known¹⁸ characteristic of $\text{H} + \text{NF}_2$ chemistry in the H atom rich regime, and its presence is another indicator of the production of NF_2 in the system.

From comparison of the rate constants for the H atom reactions with NCl_3 , NFCl_2 , and NF_3 , the $\text{H} + \text{NF}_2\text{Cl}$ reaction is expected to have a rate constant on the order of $10^{-12} \text{ cm}^3 \text{ s}^{-1}$ or less. For the reagent densities in our discharge-flow experiments, on the order of 10^{13} cm^{-3} , the time constant for the rate of production of $\text{NF}(a)$ (corresponding to the time decay of the $\text{NF } a \rightarrow X$ intensity in the reactor) should be 100 ms or greater. This was indeed the case. Consequently, we were unable to accurately determine this rate constant in these experiments. To address this issue, we performed a number of preliminary experiments based on pulsed laser initiation of the reaction. In these experiments, mixtures of H_2S and NF_2Cl , heavily diluted in argon, were photolyzed at 249 nm. At this wavelength, the H_2S is photodissociated¹⁸ to produce translationally excited H atoms which are rapidly thermalized in the argon bath. These atoms react with the NF_2Cl (present in large excess) to produce vibrationally excited HCl , which emits in the IR near $3.4 \text{ } \mu\text{m}$. Figure 9 shows a time profile of HCl IR emission obtained in this manner. The rise and decay of the time profile correspond to the rate of HCl formation and the rate of its collisional quenching, respectively. Preliminary analysis of such time profiles for varying NFCl_2 densities has indicated a rate constant for the $\text{H} + \text{NF}_2\text{Cl}$ reaction near 7×10^{-13}

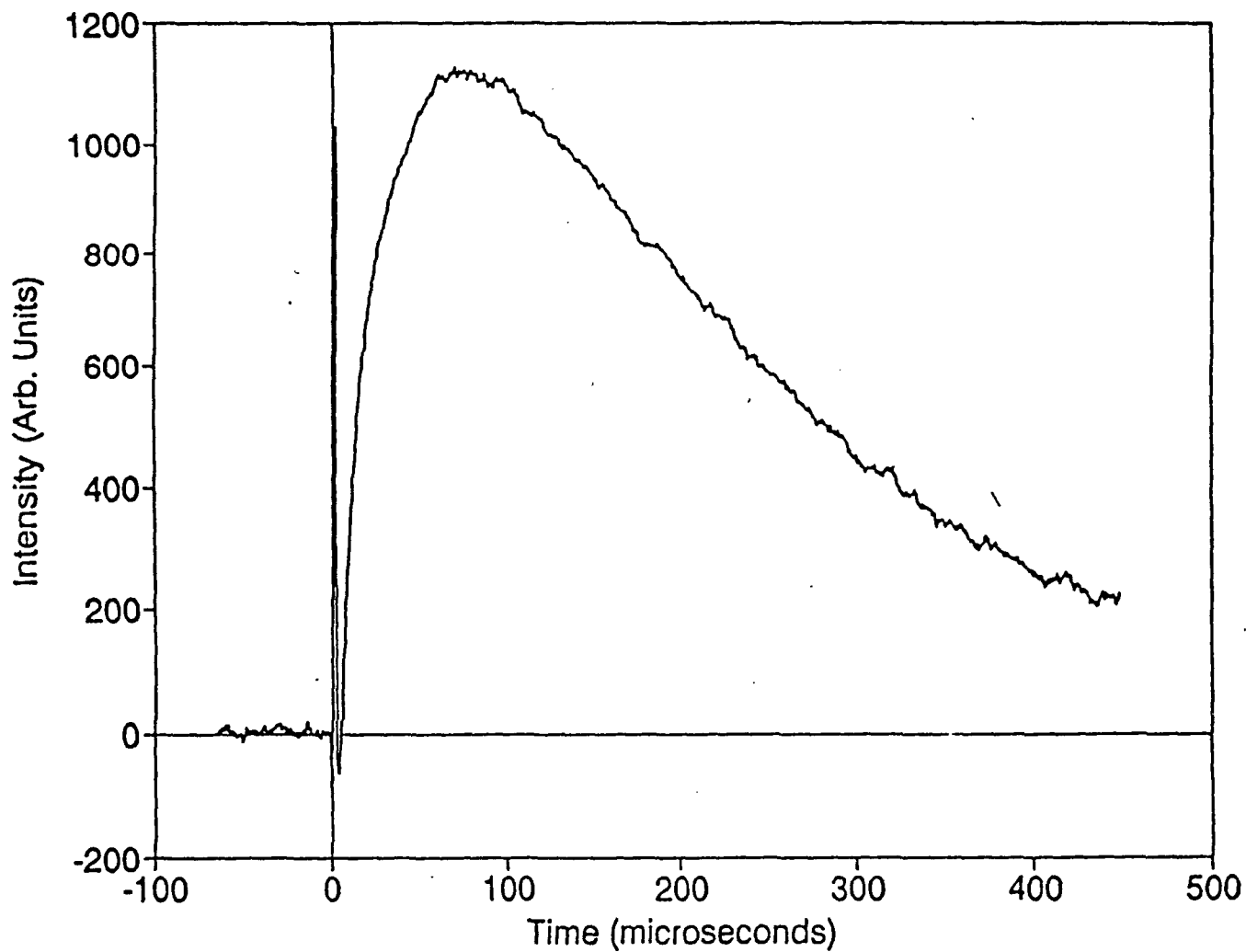


Figure 9. Time profile of IR chemiluminescence from vibrationally excited NCl produced by the $\text{H} + \text{NF}_2\text{Cl}$ reaction. Data obtained from pulsed photolysis of $\text{H}_2\text{S}/\text{NF}_2\text{Cl}/\text{He}$ mixture at 193 nm.

$\text{cm}^3 \text{ s}^{-1}$. We stress that this is a preliminary result which must be refined from additional data. Nonetheless, it shows that this pulsed method is a useful means to probe the rates of these reactions.

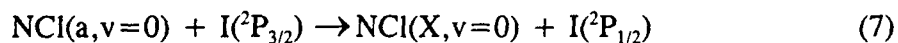
The $\text{H} + \text{NF}_2\text{Cl}$ reaction has also been studied in Setser's laboratory at Kansas State University. It was observed that the reaction does indeed generate HCl exclusively (i.e., there is no branch to $\text{NFCI} + \text{HF}$), and the inverted vibrational population distribution in the HCl indicated that the reaction proceeds by an abstract mechanism.

V. Reactions and Energy Transfer Processes of Excited Nitrenes

1. Energy Transfer from $\text{NCl}(a^1\Delta)$ to Iodine Atoms

The work described above has shown that halogen amines are good sources of $\text{NF}(a)$ and $\text{NCl}(a)$ metastables. One of the primary uses of these species is as energy transfer agents for the excitation of species which may lase in the visible or near IR. For example, Bower and Yang¹⁹ have reported that energy transfer from $\text{NCl}(a)$ to iodine atoms is rapid and efficiently produces $\text{I}(^2\text{P}_{1/2})$. We have shown that this process occurs readily when iodine sources are admitted to either the $\text{H} + \text{NFCI}_2$ or $\text{H/D} + \text{NCl}_3$ reaction media, and we have demonstrated¹⁵ initial density scaling of the $\text{D/NCl}_3/\text{I}$ system under the auspices of a grant funded by SDIO/IST and managed by AFOSR (grant no. AFOSR-90-0296).

As a part of the present AFOSR grant, we have made measurements of the rate constant of the excitation process:



The experiments were based on pulsed photolysis of CH_2I_2 at 193 nm to generate iodine atoms. Pence, Baughcum, and Leone²⁰ have reported that the quantum yield for $\text{I}(^2\text{P}_{1/2})$ production in this process is only 5%. In our experiments, we assumed that production of ground state iodine atoms accounts for the remaining 95%. The absorption cross section²⁰ for CH_2I_2 at this wavelength is very large ($1.24 \times 10^{-17} \text{ cm}^2$), and photolysis at the fluences employed (30 to 80 mJ/cm^2) results in dissociation of the majority of the sample. In our experiments, emission at $1.315 \text{ }\mu\text{m}$ from the $\text{I}(^2\text{P}_{1/2})$ produced from this photodissociation was monitored with a 0.275 m monochromator and liquid nitrogen cooled germanium detector. Figure 10a shows a typical time profile of this emission. It decays over more than 1 ms, likely from quenching by I_2 present as an impurity.

Under selected conditions, 193 nm photolysis of $\text{CH}_2\text{I}_2/\text{ClN}_3/\text{He}$ produces sufficient densities of both $\text{NCl}(a^1\Delta)$ and $\text{I}(^2\text{P}_{3/2})$ such that the production of $\text{I}(^2\text{P}_{1/2})$ by their interaction is readily observed. A summary of typical experimental parameters is given in Table II below, and corresponding data are shown in Figure 10 b - d. When ClN_3 is present in the mixture, the $\text{I}(^2\text{P}_{1/2})$ emission exhibits a rise over several hundred μs to peak intensities much greater than that produced by photolysis of the CH_2I_2 alone. The presence of both CH_2I_2 and ClN_3 in the mixture was required for observation of this emission. Figure 11a shows the time profile of the iodine emission over several ms. The $\text{I}(^2\text{P}_{1/2})$ produced initially by photolysis of CH_2I_2 is clearly evident by its abrupt rise, separated from the slower rise of the much more intense emission excited by collisions with $\text{NCl}(a)$. Figure 11b shows the time profile of $1.08 \text{ }\mu\text{m}$ emission from the $a^1\Delta, v=0 \rightarrow X^3\Sigma, v=0$ transition of NCl , from the photolysis of ClN_3/Ar alone.²¹ Clearly,

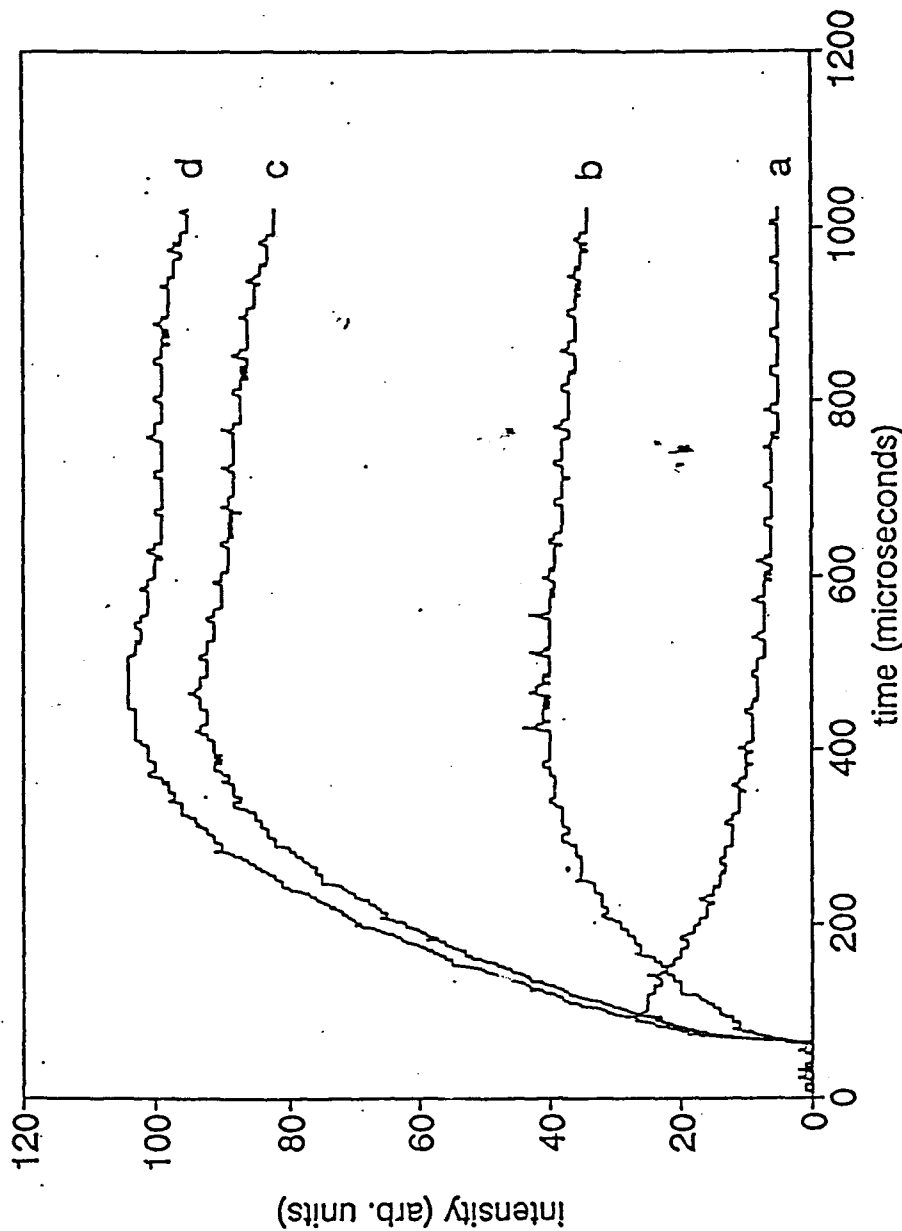


Figure 10. a). $I(2p_{1/2})$ Time Profile from 193 nm Photolysis of CH_2I_2 at 59 mJ/cm^2 . b), c), d). $I(2p_{1/2})$ Emission Time Profiles from Photolysis of CH_2I_2/ClN_3 Mixtures at 30, 67, and 76 MJ/cm^2 Respectively.

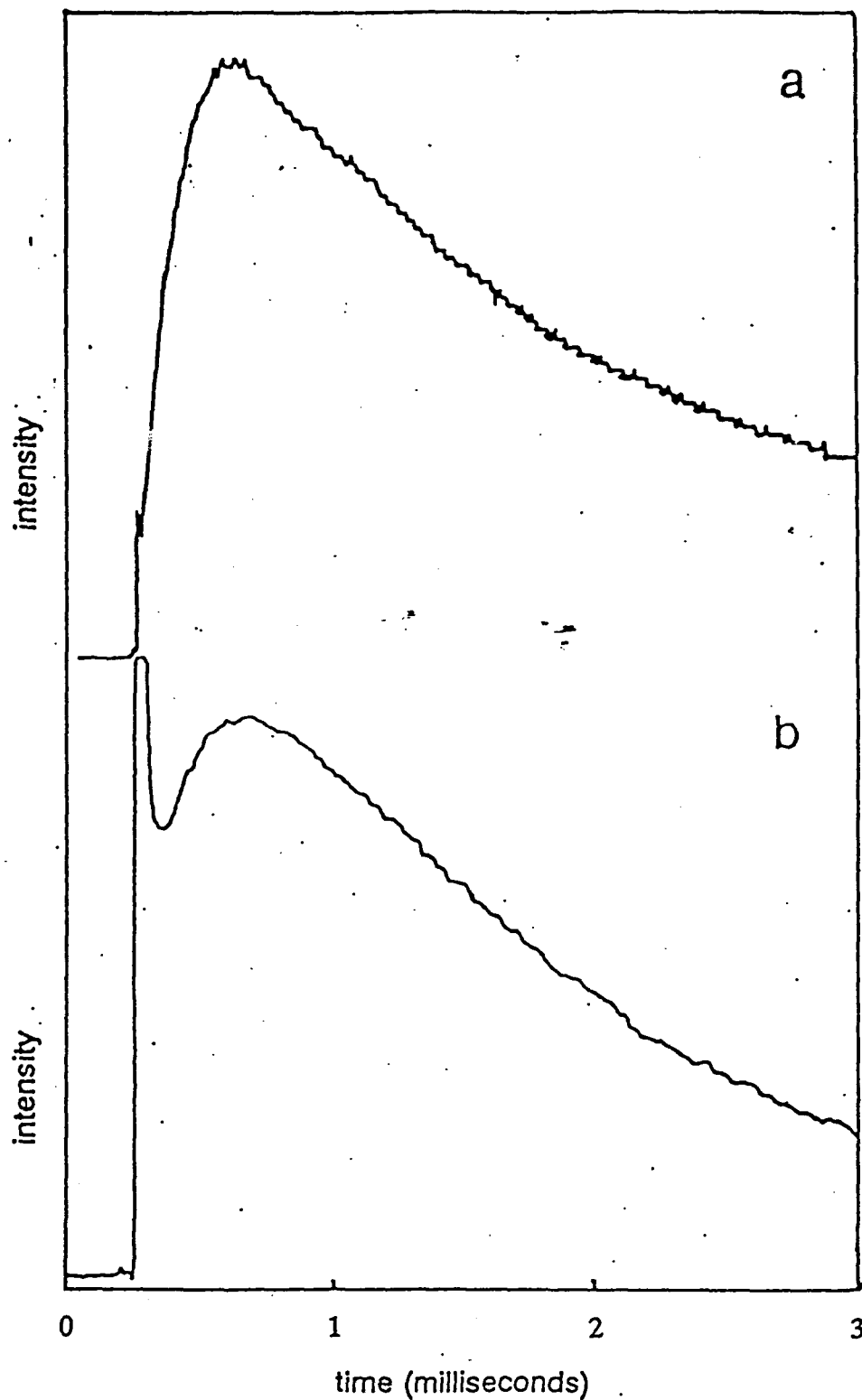


Figure 11. a). Time Profile of $I(2P_{1/2})$ Emission from 193 nm Photolysis of a CH_2I_2/ClN_3 Mixture.
 b). Time Profile of $NCl(a, v=0)$ from Photolysis of ClN_3 Alone, under Comparable Conditions.

the time profile of the iodine emission from $\text{ClN}_3/\text{CH}_2\text{I}_2/\text{Ar}$ tracks the $\text{NCl}(a, v=0)$ signal from photolysis (proportional to the density of $\text{NCl}(a, v=0)$) with its decay rate being rapid and

Table II. Typical Experimental Parameters for $\text{CH}_2\text{I}_2/\text{ClN}_3$ Photolysis at 193 nm and 76 mJ/cm²

Species	$\alpha(\text{cm}^2)$	$\rho(\text{initial}), \text{cm}^{-3}$	$\rho_0(\text{after photolysis}), \text{cm}^{-3}$
CH_2I_2	1.24×10^{-17}	3.5×10^{14}	4.2×10^{13}
ClN_3	1.38×10^{-18}	8.5×10^{15}	6.7×10^{15}
$\text{NCl}(a^1\Delta)$			1.8×10^{15}
$\text{I}(^2\text{P}_{3/2})$			2.9×10^{14}
$\text{I}(^2\text{P}_{1/2})$			1.5×10^{13}

roughly constant.

A steady state condition therefore holds when the $\text{I}(^2\text{P}_{1/2})$ time profile is relatively flat after the rise (see Figure 10). At the steady state,

$$[\text{I}(^2\text{P}_{1/2})] = \frac{k[\text{I}(^2\text{P}_{3/2})][\text{NCl}(a)]}{k_Q[\text{Q}]} \quad (8)$$

where k is the rate constant for $\text{I}(^2\text{P}_{1/2})$ production by collisions with $\text{NCl}(a)$ and k_Q is the rate constant for its quenching by species Q present in the mixture. From the time profile in Figure 10a, quenching by CH_2I_2 and its photoproducts is clearly too slow to contribute significantly to the total quenching rate when ClN_3 is present. On the other hand, quenching by ClN_3 is

expected to be rapid. Assuming ClN_3 to be the primary quencher, eqn. 8 is rearranged as follows:

$$k = \frac{k_Q[I(^2P_{1/2})][\text{ClN}_3]}{[I(^2P_{3/2})][\text{NCl(a)}]} \quad (9)$$

where the densities shown are the values at the steady state as described above. The value of k_Q was determined by explicit measurements of $I(^2P_{1/2})$ quenching by ClN_3 , in experiments in which the $I(^2P_{1/2})$ time decay was measured from 249 nm photolysis of CF_3I in the presence of various densities of ClN_3 . The value of k_Q was found to be $2.0 \pm 0.3 \times 10^{-11} \text{ cm}^3 \text{ s}^{-1}$. This value allows us to calculate k , the energy transfer rate constant, from eqn. 9 since all of the remaining parameters are known from the $\text{CH}_2\text{I}_2/\text{ClN}_3/\text{Ar}$ photolysis experiments. The $I(^2P_{1/2})$ density is determined from data such as that shown in Figure 10, since an absolute calibration of the intensity scale is obtained from knowledge that the initial density corresponds to 5% of the CH_2I_2 photoproducts. The density of $I(^2P_{1/2})$ can then be corrected for the density that has been pumped to the $^2P_{1/2}$ state at the steady state.

Many experiments were performed in which data similar to that shown in Figure 10 were obtained for a variety of CH_2I_2 and ClN_3 densities and laser fluences. Taken all together, these data indicated a rate constant $k = 1.8 \pm 0.3 \times 10^{-11} \text{ cm}^3 \text{ s}^{-1}$. It is important to note that this value corresponds to the rate constant for excitation of iodine atoms to the $^2P_{1/2}$ state, not to overall quenching of NCl(a,v=0) by iodine atoms.

Apart from determination of the energy transfer rate constant, a number of interesting observations are made from these data. First, it is clear that the quenching of $I(^2P_{1/2})$ by ClN_3 and NCl(a) by iodine atoms are both very much faster than the time profiles in Figure 11. Some

mechanism which regenerates these species must be at work in the system. We postulate that this mechanism involves dissociation of ClN_3 in the quenching of excited iodine:



Such a process is not at all unreasonable. The barrier for ClN_3 dissociation to $\text{NCl(a)} + \text{N}_2$ is thought to be only about 16 kcal/mole,¹¹ considerably less than the energy carried by $\text{I}(^2\text{P}_{1/2})$, and Benard and co-workers¹¹ have shown that substantial densities of NCl(a) can be produced by thermolysis of ClN_3 . Further information concerning this issue has been obtained during the course of measurements of rate constants for NCl(a) quenching by a number of collision partners. These data are described below. Another interesting point is that the excitation of iodine by NCl(a) is surely very efficient, even at moderate densities such as those in our experiments. For the data in Figure 10d, approximately 25% of the total iodine atoms present are in the $2\text{P}_{1/2}$ state, close to a population inversion (which requires that one third of the atoms be in the excited state). This certainly bodes well for the development of iodine lasers based on energy transfer from NCl(a) in either pulsed photochemical systems or chemical generators such as the amine systems described above.

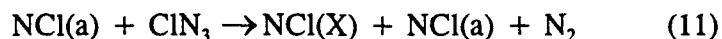
2. $\text{NCl(a}^1\Delta)$ Quenching by Diatomics

During the course of this program, it became apparent that interpretation of data from discharge-flow experiments on amine systems or pulsed experiments on isocyanate or azide systems requires some knowledge of rates of collisional quenching of excited NCl(a) . Although rate constants for analogous quenching of NF(a) by a wealth of collision partners are known,²² little or no information exists concerning quenching of excited NCl . An exception is the early

work by Clyne and co-workers²³ in which rate constants for quenching by Cl₂ and O₂ were inferred from discharge-flow experiments. These authors used a mass spectrometer to monitor NCl₂, which was thought to be a product of NCl(a) reaction with Cl₂. For appropriate conditions, the NCl₂ time dependence should reflect that of the original NCl(a). Other than these numbers no information was available prior to our work in this area.

The objective of this project was to measure rate constants for NCl(a) quenching by a number of diatomics present in the halogen amine systems. This work was undertaken under the joint auspices of this AFOSR program and a parallel program funded by SDIO/IST, "Reactions and Spectroscopy of Excited Nitrenes," (F496F20-92-J-0270). None of the data obtained to date has yet been published. The work continues under the ongoing SDIO/IST program.

The experiments were based on generation of NCl(a) by pulsed photolysis of ClN₃ at 249 nm. Quenching of the NCl(a) by the parent ClN₃ is a significant issue, both because it is rapid and because we believe it sets up a chain which extends dramatically the NCl(a) time profile. Processes analogous to reaction (10) above may occur, in which NCl(a) is quenched by ClN₃ but is regenerated by the subsequent ClN₃ dissociation:



Evidence of such a chain is found in a very long low intensity "tail" to the decay of NCl(a) from ClN₃ photolysis, which can extend to nearly 100 ms. To avoid these issues, the ClN₃ density in the quenching experiments was kept low, at 10¹⁴ cm⁻³ or less. In this case, the overall NCl(a) decay (in the absence of added species) is dominated by diffusion to the walls of the 2.54 cm

diameter photolysis cell. This diffusion rate could be easily varied by the pressure of He diluent. Typical experiments were performed at a total pressure near 6 Torr, such that the observed NCl(a) decay time was on the order of 300 μ s. The decays for such conditions were nicely exponential with very little evidence of the long tail.

Rate constants for quenching by various gases were determined by simply admitting various amounts of these species to the flow, taking care to ensure that the total pressure remained constant. The quenching rates for these species were typically large enough that only small flows (and hence minimal corrections of the diluent flow to maintain constant pressure) were necessary to observe substantial changes in the decays. Rate constants were determined from plots of the exponential decay rate of the 1.08 μ m emission vs. the density of the added quencher. In all cases studied thus far, these plots have been quite linear, the slopes yielding the quenching rate constants. Figure 12 shows a plot for quenching by O₂. Table III shows the rate constants measured to date, for quenching by Cl₂, O₂, H₂, D₂, HCl, and Ar. We are currently synthesizing DCl in order to measure a rate constant for this species. It is important to note that these rate constants are for quenching of NCl(a, v=0). Only emission from the 0,0 band of the NCl a \rightarrow X transition was transmitted by the narrow band filter mounted in front of the cooled Ge detector used in these experiments.

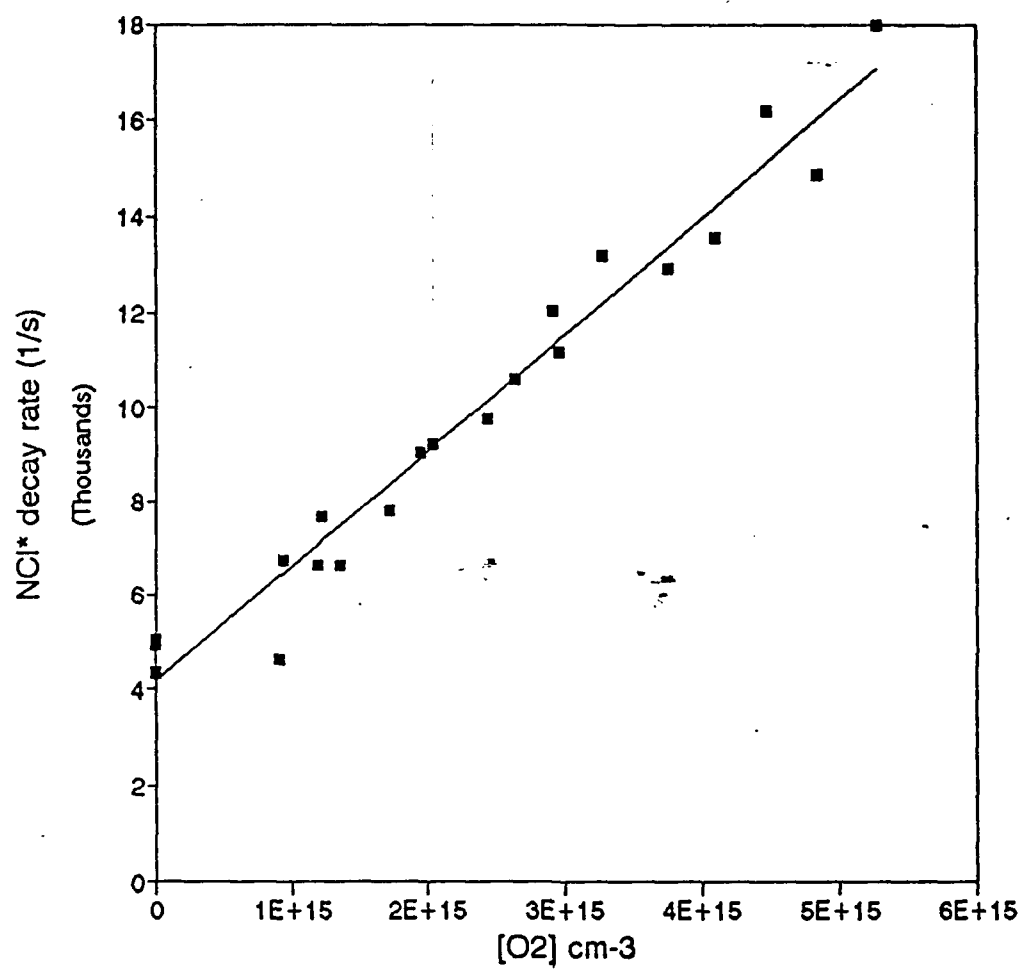


Figure 12. Exponential Decay Rate of NCl(a, v=0) vs. the Density of Added O₂.

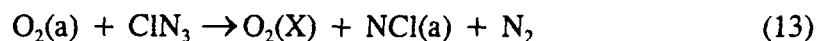
Table 3. Rate Constants for Quenching of $\text{NCl}(a^1\Delta, v=0)$ by Diatomic Molecules and Atoms

Quencher	$k(\text{cm}^3\text{s}^{-1})$
Ar	$1.2 \pm 0.5 \times 10^{-14}$
Cl_2	$1.8 \pm 0.3 \times 10^{-11}$
O_2	$2.5 \pm 0.2 \times 10^{-12}$
HCl	$4.9 \pm 0.7 \times 10^{-12}$
H_2	$6.8 \pm 0.7 \times 10^{-13}$
D_2	$5.3 \pm 0.6 \times 10^{-13}$

$\text{NCl}(a)$ quenching by O_2 is expected to be dominated by an E to E mechanism in which the O_2 is excited to its $a^1\Delta_g$ state:

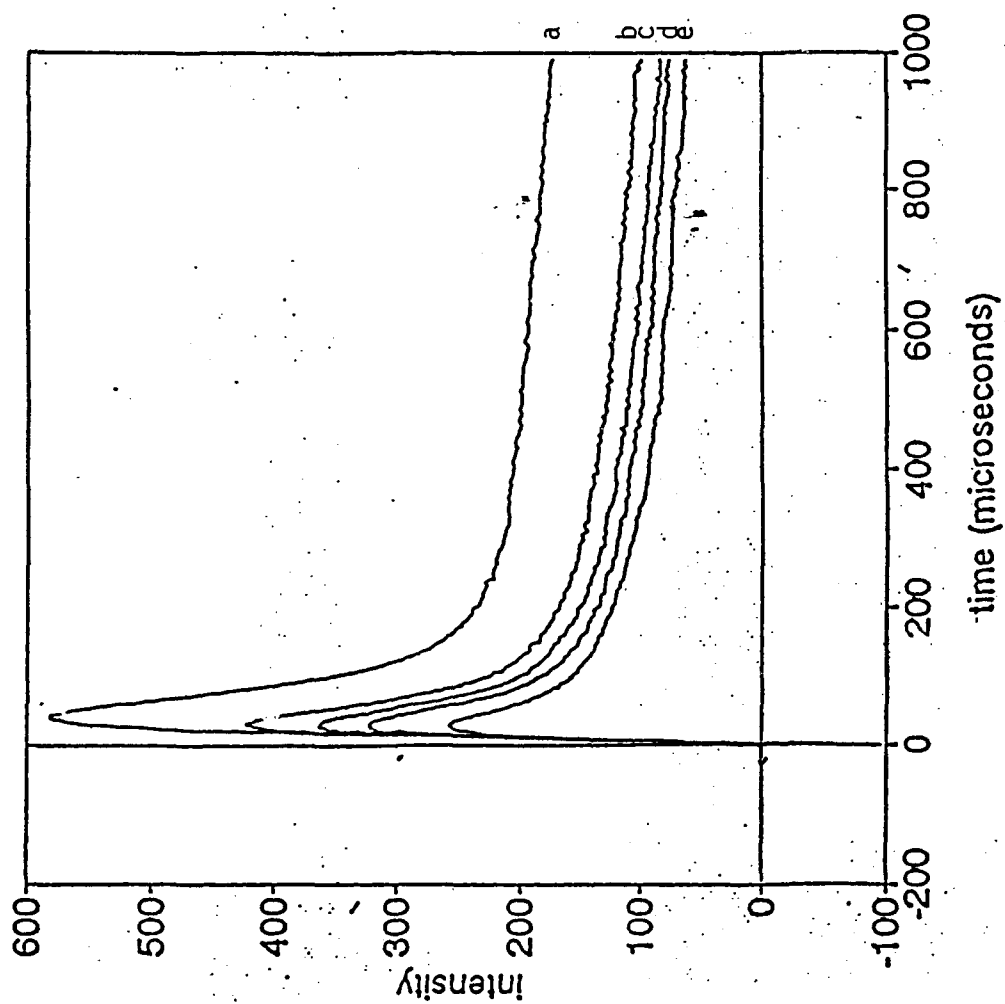


For production of $\text{O}_2(a, v=0)$ this process is exothermic by 1400 cm^{-1} . It seems more likely (particularly in view of the magnitude of the rate constant) that $\text{O}_2(a)$ is formed in the $v=1$ state, a process which is near resonant with an endothermicity of 87 cm^{-1} . When ClN_3 is present in larger density, it might be dissociated by $\text{O}_2(a)$ just as it might by $\text{NCl}(a)$ or $\text{I}(^2\text{P}_{1/2})$:



Processes (12) and (13) form a chain carried by $\text{NCl}(a)$ and $\text{O}_2(a)$ which results in the overall removal of the ClN_3 from the system.

Evidence of the operation of this chain is found when ClN_3/O_2 mixtures are photolyzed at higher ClN_3 densities. Figure 13a shows the time decay of $\text{NCl}(a)$ produced by 249 nm



$[\text{ClN}_3] = 3.8 \times 10^{14} \text{ cm}^{-3}$

249 nm photolysis

$[\text{O}_2] \text{ cm}^{-3}$	Total Pressure (Torr)
0	0.62
8×10^{14}	0.73
1.5×10^{15}	0.84
1.9×10^{15}	0.90
3.8×10^{15}	1.20

Figure 13. a). Time Profile of Emission from NCl ($a, v=0$) from 249 nm Photolysis of ClN_3 . b), c), d), e). Time Profiles with Added O_2 at Densities Shown in the Table at Right.

As O_2 is added (Figure 12 b - e), the intensity of the tail is diminished but there is little effect on its time decay. If it is assumed that the chemistry is dominated by reactions (12) and (13), then at the steady state

$$\frac{k_{13}}{k_{12}} = \frac{[NCl(a)][O_2(X)]}{[O_2(a)][ClN_3]} \quad (14)$$

If $NCl(a)$ is converted to $O_2(a)$ with unit efficiency, then the density of $O_2(a)$ is proportional to the reduction in the intensity of the $NCl(a)$ emission, and the $NCl(a)/O_2(a)$ ratio can be inferred from the data to solve eqn. 14 for k_{13} . From this analysis, k_{13} is found to be on the order of $10^{-10} \text{ cm}^3 \text{ s}^{-1}$, indicating a very rapid process.

The rate constants for quenching by H_2 and D_2 shown in Table III are most unexpected. First, there is no isotope effect. In studies of the generation of $NCl(a)$ and $I(^2P_{1/2})$ in a transverse flow reactor,¹⁵ $D + NCl_3$ was found to perform approximately five times better than $H + NCl_3$. Further, the magnitudes of the rate constants are much greater than expected based on the flow reactor data. The densities of H_2 or D_2 used in the reactor were such that, if these rate constants are correct, the vast majority of the $NCl(a)$ should have been quenched. Instead, $NCl(a)$ densities as high as 10^{13} cm^{-3} were observed with a roughly 10% yield relative to the initial NCl_3 flows. This remains a mystery. The H_2 and D_2 quenching measurements were repeated four times in light of this question; the results of each of the measurements were consistent with the data shown in Table III. It may be that quenching by HCl or DCl is responsible for the isotope effect observed in the reactor. Our measurement with DCl will seek to test this point.

3. Reactions of $\text{NH}(a^1\Delta)$ with Molecular Halogens

The dynamics of processes involving the imidogen radical are of considerable interest because of the relatively simple structure of this species and its tractability as a subject for computational study. Previously in our laboratory, we have studied reactions of the isoelectronic species $\text{O}(^1\text{D})$ with HN_3 ,²⁴ HNCO ⁶ and ClNCO .²⁵ These processes were observed to proceed by either insertion or direct abstraction mechanisms. The reactions of $\text{NH}(a^1\Delta)$ with molecular halogens may proceed by insertion or abstraction in an analogous manner, as follows:



The insertion process, reaction 16, is particularly interesting since its dihaloamine-like intermediate may be very similar to that of the $\text{H} + \text{NX}_2$ reactions described above. If so, the insertion process would be expected to produce $\text{NX}(a^1\Delta)$ and vibrationally excited HX . For example, the $\text{NH}(a^1\Delta) + \text{Cl}_2$ reaction may have a similar transition state to $\text{H} + \text{NCl}_2$. In this case, the insertion mechanism analogous to reaction 16 is exothermic by 63 kcal/mole, easily sufficient to produce $\text{NCl}(a)$ and HCl with considerable vibrational excitation.

In our initial effort on this project, we measured the rate constant for $\text{NH}(a^1\Delta)$ quenching by Cl_2 and determined the dominant product channels. The experiments involved photolysis of mixtures of HN_3 , Cl_2 , and argon with pulsed radiation at 249 nm from a KrF laser. At this wavelength, the HN_3 is dissociated²⁶ to $\text{NH}(a^1\Delta)$ and N_2 , while photodissociation of the Cl_2 is negligible. The flowing reagent gases were allowed to mix just upstream of the pyrex photolysis cell, and no evidence of pre-reaction was observed for these conditions. $\text{NH}(a^1\Delta)$ was observed

by LIF on the $a^1\Delta - c^1\Pi$ transition of this radical²⁷ near 325 nm. Time resolution of the $NH(a^1\Delta)$ density was obtained by varying the delay time between the 249 nm photolysis pulse and the LIF probe. The time decays were found to be exponential, becoming much shorter as the density of Cl_2 in the flow increased. Figure 14 shows a typical plot of the exponential $NH(a^1\Delta)$ decay rate vs. the Cl_2 density. The intercept at $[Cl_2] = 0$ agrees well with the well known²⁷ rate constant for $NH(a^1\Delta)$ quenching by HN_3 . Nine sets of data such as that shown in Figure 14 were obtained, with consistent results. From the slopes of these plots, a rate constant $k = 6.8 \pm 0.4 \times 10^{-11} \text{ cm}^3 \text{ s}^{-1}$ was obtained for the overall quenching of $NH(a^1\Delta)$ by Cl_2 . This rate constant is far too large to include a significant contribution from E to V,R or E to T processes, and we expect that chemical reaction dominates the quenching mechanism.

The products of the reaction were sought by their characteristic emissions. Emission from vibrationally excited HCl was readily observed with a filter transmitting near $3.4 \mu\text{m}$ and a cooled InSb detector. The time profile of the emission showed a fast rise corresponding to the rate of the reaction followed by a somewhat slower decay corresponding to $HCl(v)$ collisional relaxation. Emission from the $NCl(a \rightarrow X)$ transition near $1.03 \mu\text{m}$ was observed with a narrowband filter at this wavelength and a cooled Ge detector. Figure 15 shows a typical time profile of the $NCl(a^1\Delta)$ emission, corrected for background. The background (less than 20% of the $NCl(a)$ signal) was due largely to emission from excited NH_2 produced by reaction²⁷ of $NH(a)$ with the parent HN_3 . The observed time profile of the $NCl(a)$ emission is distorted by the finite time constant of the Ge detector, about $13 \mu\text{s}$.

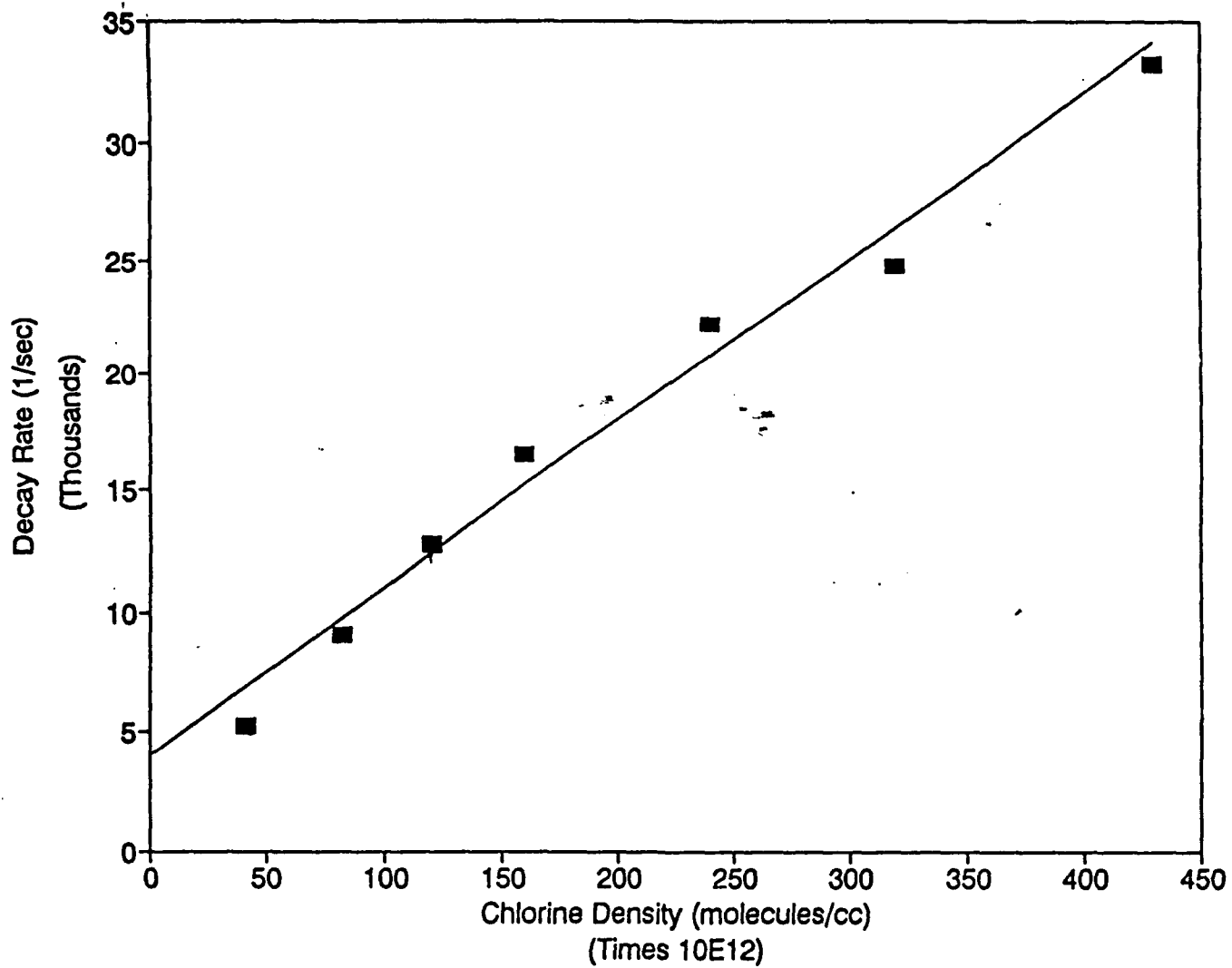


Figure 14. Exponential Decay Rate of $\text{NH}(a^1\Delta)$ vs. the Density of Added Cl_2 .

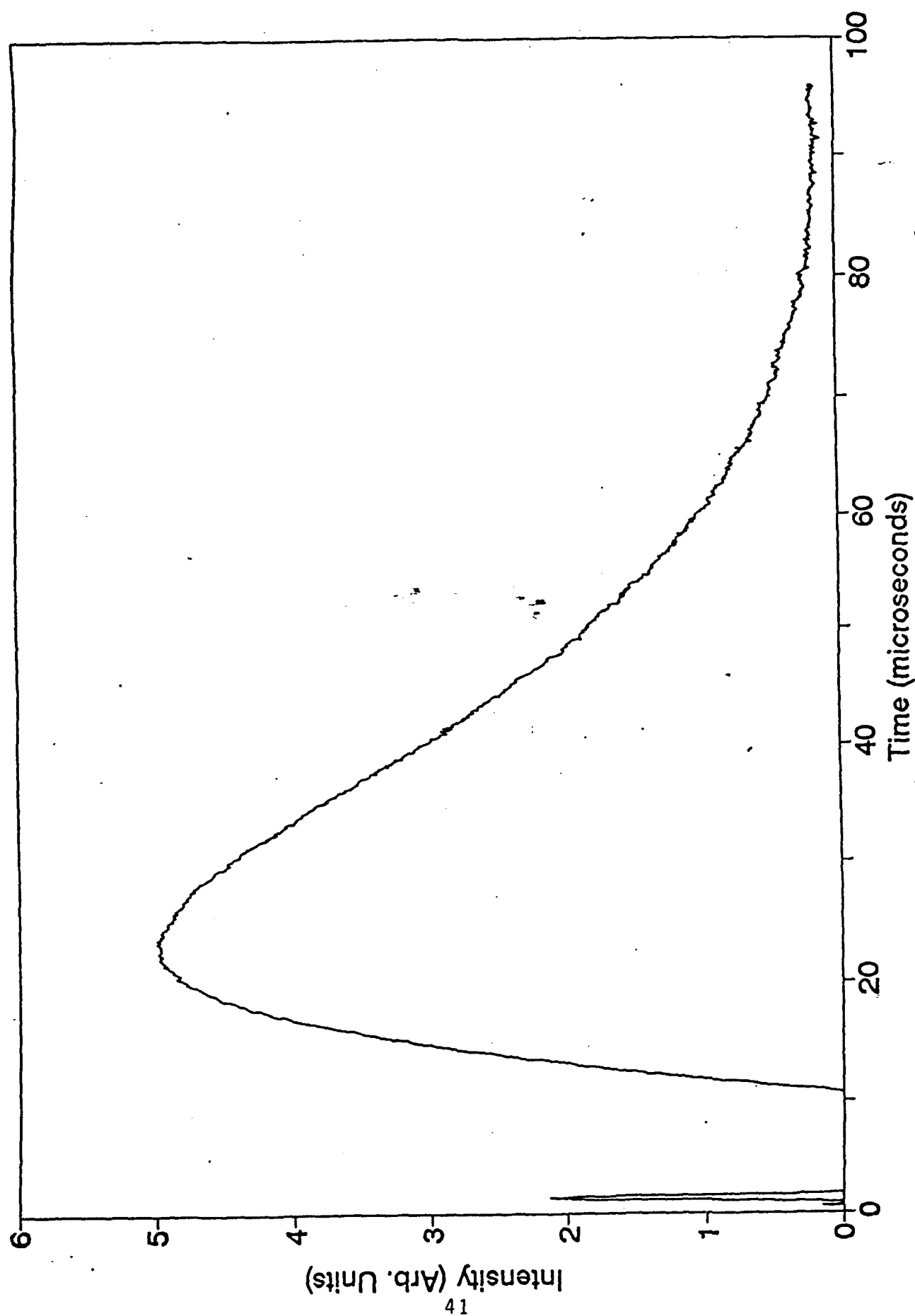


Figure 15. Time Profile of $\text{NCl}(a^1\Delta, v=0)$ Produced by the Reaction of $\text{NH}(a^1\Delta)$ with Cl_2 .

A number of experiments were performed in an effort to determine whether the production of excited NCl(a) via the insertion mechanism is a major channel for the reaction. This was done by comparing the intensity of the $\text{NCl(a)} \rightarrow \text{X}$ emission from the reaction with that from photolysis of ClN_3 at 249 nm. From comparison with the photochemistry of other azides, it is expected that the yield of $\text{NCl(a}^1\Delta)$ from ClN_3 photolysis at this wavelength is very high, if not unity. To make this measurement, it was necessary to correct the NCl(a) intensity produced by the $\text{NH(a)} + \text{Cl}_2$ reaction for the time constant of the detector. This was done by explicitly measuring the attenuation of input pulses of varying time width by the detector. The true rise time of the NCl(a) signal was known from the rate constant of the reaction and the reagent densities. These tests indicated that the NCl(a) intensity was distorted to about 40% of its true intensity by the detector. Using this correction factor and the measured intensities, it was determined that the yield of NCl(a) produced by the reaction is nearly equivalent to that produced by 249 nm photolysis of ClN_3 . Clearly, the insertion mechanism is the dominant channel in the $\text{NH(a}^1\Delta) + \text{Cl}_2$ reaction.

The success of this experiment indicates great promise for investigating these reactions and the analogous $\text{H} + \text{NX}_2$ or $\text{H} + \text{NXY}$ reactions using this pulsed method. We have already begun to study the $\text{NH(a}^1\Delta)$ reactions with F_2 and ClF , which should be analogous to the $\text{H} + \text{NF}_2$ and $\text{H} + \text{NFCI}$ processes. We hope to resolve the vibrational distribution of the product hydrogen halides and the branching fractions between competing processes (e.g., formation of NCl or NF in the reaction with ClF) in order to make a finer comparison with similar data from the $\text{H} + \text{aminyl}$ radical reactions.

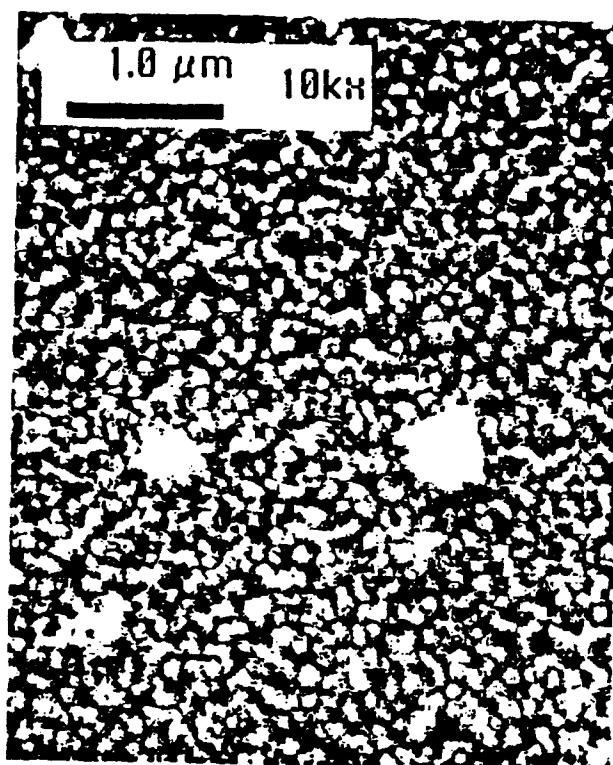
VI. Photochemical Deposition of IIB -VI Thin Films

This is a new project based on old data. Some years ago, an undergraduate researcher in our laboratory (M.P. Gelinas) measured rate constants for quenching of metastable excited $\text{Zn}(^3\text{P})$ atoms by a number of group VI molecules like H_2S , CS_2 , and O_2 . These quenching processes were found to be extremely fast, with rate constants greater than $10^{10} \text{ cm}^3 \text{ s}^{-1}$. Although the mechanisms were presumed to be reactive, producing ZnS or ZnO , the spectroscopy of these species was unknown at the time and we were unable to probe for these products. Our real interest was in making thin films, but the flashlamp-pumped dye laser used to excite the Zn atoms was woefully inadequate for this purpose (a calculation showed that many thousands of laser pulses would be required to produce a monolayer thin film in a 1 mm^2 area). The quenching data were never published. The project was resurrected under this AFOSR grant, however, after we acquired an excimer-pumped dye laser system.

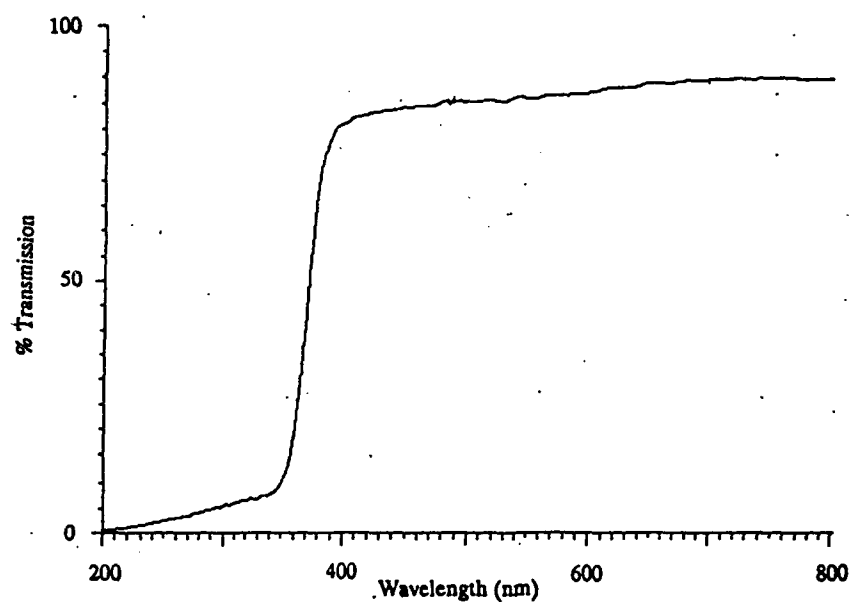
We have now succeeded in producing thin films of ZnS and ZnO by optical excitation of Zn vapor from an evaporative source followed by reaction with O_2 or CS_2 , or alternatively by sputtering Zn from a target under O_2 or CS_2 using a XeCl excimer laser. The latter method is much more efficient. In this case, the 308 nm laser radiation serves to produce atoms of Zn by sputtering, and also optically excites these species to the ^3P metastable excited state. The $^1\text{S} \rightarrow ^3\text{P}$ transition in Zn lies at 307.6 nm. The gaseous atoms are only weakly excited by the 0,0 band of the laser output, but the efficiency of excitation under sputtering conditions is much greater than expected. We believe that this is because the absorption lines of the metal atoms are broadened significantly in the vicinity of the target surface, as they pass from the band structure of the metal solid to the distinct transitions of the free atoms. The sputtered atoms leave the

surface in the radiation field of the laser, and near the surface their absorption is sufficiently broadened to efficiently absorb the radiation over its full band width. When this "near-resonant" sputtering occurs in the presence of a reactive gas, product formation leads to the deposition of a thin (or sometimes thick) film. Figure 16a shows an electron micrograph of a ZnO film deposited on a quartz substrate in this manner. Figure 16b shows a UV/visible absorption spectrum of the film, which exhibits the sharp cut-on near 380 nm characteristic of ZnO. In fact, this cut-on is characteristic of crystalline or polycrystalline ZnO, as amorphous ZnO has an optical cut-on at much lower wavelengths.²⁸ Indeed, the X-ray pattern of the film (Figure 17) shows that it is polycrystalline, with preferred c axis orientation often observed in ZnO films. ZnS films were made by sputtering Zn under CS₂. In this case the films were amorphous, but the Zn/S stoichiometry agreed well with that from a powder standard when observed with an EDAX system.

We are continuing to perform further exploratory experiments in an effort to test the potential of this new method for the deposition of a variety of IIB-VI thin films, many of which are used as photovoltaics, components of semiconductor devices, or high index optical coatings.



A



B

Figure 16. a). Electron Micrograph of ZnO Thin Film Produced by "Resonant Sputtering" of Zn under O_2 . b). UV/Visible Absorption Spectrum of the ZnO Thin Film.

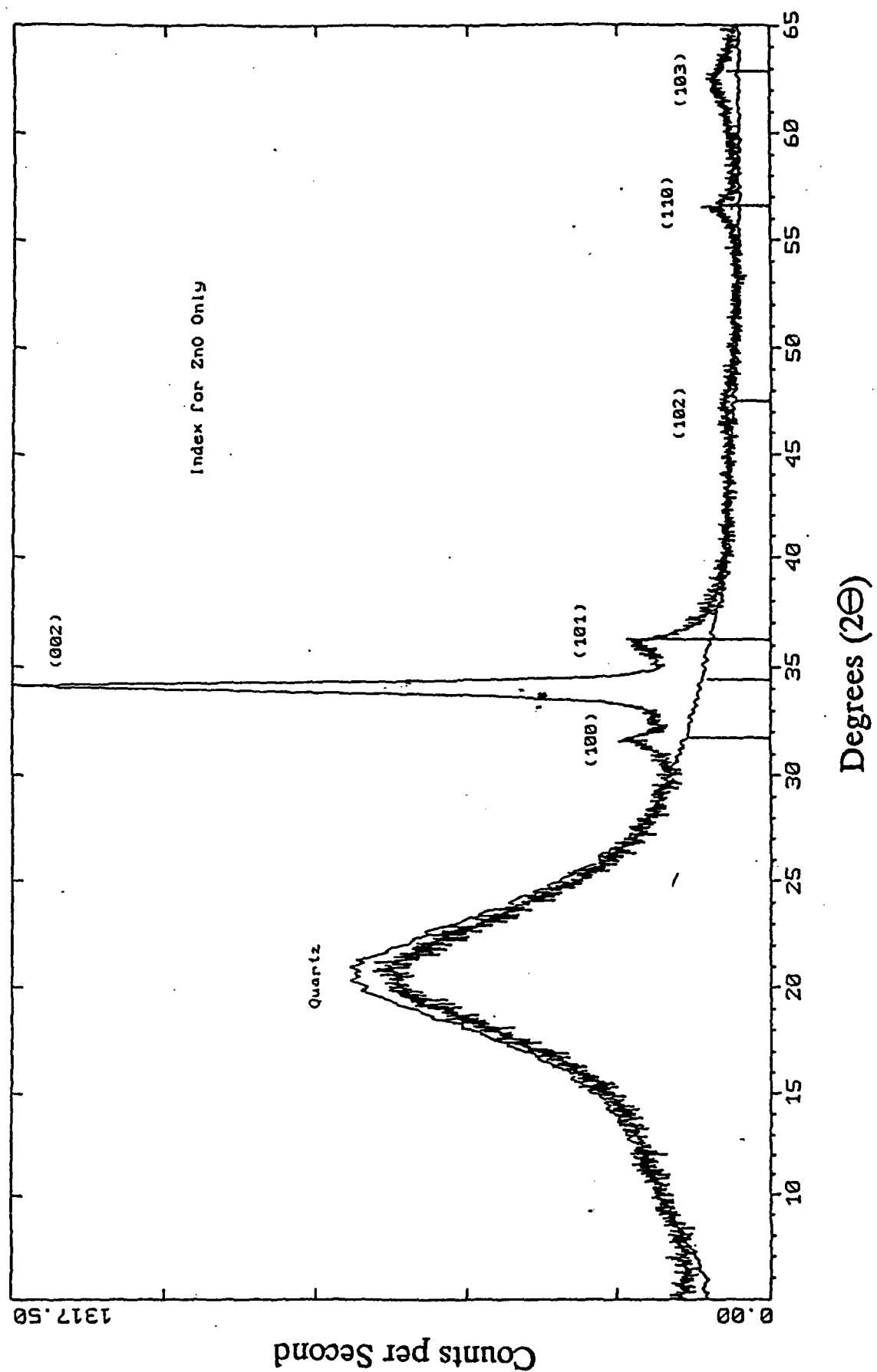


Figure 17. X-Ray Diffraction Pattern of the ZnO Produced by Resonant Laser Sputtering of Zn under O_2 , Indexed to Wurtzite Structure.

VII. Publications Arising From This Work

1. D.B. Exton, J.V. Gilbert, and R.D. Coombe, "Generation of Excited NCl by the Reaction of Hydrogen Atoms with NCl_3 ", J. Phys. Chem, **95**, 2692, (1991).
2. D.B. Exton, J.V. Gilbert, and R.D. Coombe, Kinetics and Mechanism of the Reaction of NFCI_2 with Hydrogen Atoms", J. Phys. Chem., **95**, 7758, (1991).
3. X. Liu, M.A. MacDonald, and R.D. Coombe, "Rates of Reaction of N_3 with F, Cl, Br, and H Atoms", J. Phys. Chem., **96**, 4907, (1992).
4. S.M. Singleton and R.D. Coombe, "Dynamics of the $\text{O}(^1\text{D}) + \text{ClNCO}$ Reaction", J. Phys. Chem., **96**, 9865, (1992).
5. A.J. Ray and R.D. Coombe, "Energy Transfer from $\text{NCl}(a^1\Delta)$ to Iodine Atoms", J. Phys. Chem., **97**, 3475, (1993).
6. E. Arunan, C.P. Liu, D.W. Setser, J.V. Gilbert, and R.D. Coombe, "Infrared Chemiluminescence Studies of the $\text{H} + \text{NFCI}_2$ and $\text{H} + \text{NFCI}$ Reactions", submitted to J. Phys. Chem., 1993.
7. S.M. Singleton and R.D. Coombe, "Rate and Mechanism of the $\text{NH}(a^1\Delta) + \text{Cl}_2$ Reaction", submitted to Chem. Phys. Lett., 1993.
8. Z. Liu, M.P. Gelinas, and R.D. Coombe, "II-VI Compound Thin Film Deposition by Resonant Laser Sputtering", submitted to J. Appl. Phys., 1993.

In addition to these papers and manuscripts, it is expected that a manuscript describing our work on the $\text{NCl}(a)$ collisional quenching studies (by A.J. Ray and R.D. Coombe) will be submitted to J. Phys. Chem. before the end of 1993. Also, the University of Denver is in the process of

filing a patent application based on the "resonant sputtering" method for the deposition of II-VI thin films.

VIII. Personnel

Principal Investigator: Dr. Robert D. Coombe

Senior Research Personnel (faculty collaborators);

Dr. Julanna V. Gilbert

Dr. Donald W. Setser

Postdoctoral Research Associates:

Dr. Xu Liu

Dr. Michael A. MacDonald

Graduate Research Assistants:

Deborah B. Exton *

Steven M. Singleton

Amy J. Ray

Zhiyu Liu **

* Ph.D. Awarded, June 1992

** M.S. Awarded, June 1993

IX. References

1. R.D. Coombe and A.T. Pritt, Jr., Chem. Phys. Lett., 58, 606 (1978).
2. A.T. Pritt, Jr., D Patel, and R.D. Coombe, Int. J. Chem. Kinetics, 16, 977 (1984).
3. J. Habdas, S. Wategaonkar, and D.W. Setser, J. Phys. Chem., 91, 451 (1987).
4. S.J. David and R.D. Coombe, J. Phys. Chem., 90, 3260 (1986).
5. R.A. Beamon, T. Nelson, D.S. Richards, and D.W. Setser, J. Phys. Chem., 91, 6090 (1987).
6. X. Liu, N.P. Machara, and R.D. Coombe, J. Phys. Chem., 95, 4983 (1991).
7. R.D. Coombe, D. Patel, A.T. Pritt, J., and F.J. Wodarczyk, J. Chem. Phys., 75, 2177 (1981).
8. R.F. Heiner, III, H. Helvajian, G.S. Holloway, and J.B. Koffend, J. Phys. Chem. 93, 7813 (1989).
9. D.D. Bell and R.D. Coombe, J. Chem. Phys., 82, 1317 (1985).
10. J.V. Gilbert and R.D. Coombe, J. Chem. Phys., 89, 4082 (1988).
11. See for example D.J. Benard, M.A. Chowdhury, B.K. Winker, T.A. Sedar, and H.H. Michels, J. Phys. Chem., 94, 7507 (1990).
12. See for example R.J. Malins and D.W. Setser, J. Phys. Chem. 85, 1342 (1981).
13. E. Arunan, C.P. Lin, D.W. Setser, J.V. Gilbert, and R.D. Coombe, J. Phys. Chem., submitted (1993).
14. A. Fontijn, C.B. Meyer, and H.I. Schiff, J. Chem. Phys., 40, 64 (1964).
15. R.W. Schwenz, J.V. Gilbert, and R.D. Coombe, Chem. Phys. Lett., 207, 526 (1993).
16. J. Habdas and D.W. Setser, J. Phys. Chem., 93, 229 (1989).

17. J.M. Herbelin and N. Cohen, Chem. Phys. Lett., 20, 605 (1973).
18. See for example S.R. Leone, Ann. Rev. Phys. Chem., 35, 109 (1984).
19. R.D. Bower and T.T. Yang, Opt. Soc. Amer. B, 8, 1583 (1991).
20. W.H. Pence, S.L. Baughcum, and S.R. Leone, J. Phys. Chem., 85, 3844 (1981).
21. R.D. Coombe and M.H. Van Benthem, unpublished data.
22. See for example K. Du and D.W. Setser, J. Phys. Chem., 94, 2424 (1989); 95, 4728 (1991).
23. M.A.A. Clyne, A.J. MacRobert, J. Brunning, and C.T. Cheah, J. Chem. Soc. Faraday II, 79, 1515 (1983).
24. A.P. Ongstad, R.D. Coombe, D.K. Neumann, and D.J. Stech, J. Phys. Chem., 93, 549 (1989).
25. S.M. Singleton and R.D. Coombe, J. Phys. Chem., 96, 9865 (1992).
26. B. Bohn and F. Stuhl, J. Phys. Chem., 97, 7234 (1993).
27. J.R. MacDonald, R. Miller, and A.P. Baronavski, Chem. Phys. Lett., 51, 57 (1977).
28. R.A. Mickelson and R.R. Parsons, J. Appl. Phys., 37, 3541(1966).